



## Research Article

# The treatment of acid mine drainage (AMD) using a combination of selective precipitation and bio-sorption techniques: A hybrid and step-wise approach for AMD valorization and environmental pollution control

Beauclair NGUEGANG<sup>1b</sup>, Abayneh Ataro AMBUSHE<sup>1b</sup>

Department of Chemical Sciences, University of Johannesburg, Faculty of Science, Johannesburg, South Africa

## ARTICLE INFO

### Article history

Received: 15 December 2023

Revised: 29 February 2024

Accepted: 01 April 2024

### Key words:

Acid mine drainage;  
Banana Peels; Bio-sorption;  
Environmental pollution control;  
Magnesium oxide (MgO);  
Selective precipitation

## ABSTRACT

In this study, selective precipitation using magnesium oxide (MgO) and bio-sorption with banana peels (BPs) were explored for the treatment and valorization of acid mine drainage (AMD). The treatment chain comprised two distinct stages of which selective precipitation of chemical species using MgO (step1) and polishing of pre-treated AMD using BPs (step 2). In stage 1, 2.0 L of AMD from coal mine was used for selective precipitation and recovery of chemical species using MgO. The results revealed that chemical species of concern were precipitated and recovered at different pH gradients with Fe(III) precipitated at pH ≤4, Al at pH ≥4–5, Fe(II), Mn and Zn at pH ≥8 while Ca and SO<sub>4</sub><sup>2-</sup> were precipitated throughout the pH range. In stage 2, the pre-treated AMD water was polished using BPs. The results revealed an overall increase of pH from 1.7 to 10, and substantial removal of chemical species in the following removal efficiency: Al, Cu and Zn (100% each), ≥Fe and Mn (99.99% each), ≥Ni (99.93%), and ≥SO<sub>4</sub><sup>2-</sup> (90%). The chemical treatment step removed pollutants partially, whereas the bio-sorption step acted as a polishing stage by removing residual pollutants.

**Cite this article as:** Nguegang B, Ambushe AA. The treatment of acid mine drainage (AMD) using a combination of selective precipitation and bio-sorption techniques: A hybrid and step-wise approach for AMD valorization and environmental pollution control. Environ Res Tec 2024;7(3)313–334.

## INTRODUCTION

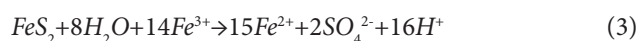
Acid mine drainage (AMD) is mine acidic by-product, containing elevated concentrations of metals and sulphate ions (SO<sub>4</sub><sup>2-</sup>) and generated by active and abandoned mines, mostly coal and gold mines [1, 2]. Specifically, AMD is formed following the oxidation of sulphide bearing materials such as pyrite (FeS<sub>2</sub>), arsenopyrite (FeAsS) and marcasite in contact with water [3]. Pyrite (FeS<sub>2</sub>) is at the forefront of AMD formation process while the contribution of other sulphide bearing materials is negligible. As such, the AMD formation process can be summarized as illustrated in equation (1), (2) and (3).



The oxidation of FeS<sub>2</sub> in the presence of water and oxygen leads to the formation of SO<sub>4</sub><sup>2-</sup>, ferrous ion [Fe(II)], and hydrogen ion (H<sup>+</sup>) equation (1). Once formed, Fe(II) is continuously oxidized to form ferric ion [Fe(III)] as illustrated in equation (2).



The Fe(III) produced after equation (2) can later oxidize FeS<sub>2</sub> to generate more Fe(II) and more H<sup>+</sup> as shown in equation (3).



\*Corresponding author.

\*E-mail address: aambushe@uj.ac.za



The above-described chemical reactions occur spontaneously or can be merely mediated or stimulated by microorganisms (sulphate and iron oxidizing bacteria) with the net effect to produce more  $H^+$  thereby increasing the acidity of the final product water [4]. Once formed, AMD becomes a matter of great environmental and human health concern and specifically in countries with intensive mining industry due to the presence of toxic chemical species that include metalloids such as arsenic (As), radionuclide such as uranium (U) and potentially toxic elements (PTEs) [5]. To be more precise, AMD is characterised by low pH ( $\leq 4.5$ ), high concentration of major metals (Al, Fe, and Mn), very high concentration of  $SO_4^{2-}$ , low concentration of Cu, Ni, Zn and Pb and trace content of alkali earth metals such as Ca and Mg [6, 7]. This acidic water has the ability to cause undesirable eco-toxicological effects on different environmental compartments and severe human health effects, which include skin irritation, kidney damage, and neurological diseases amongst others [5, 8]. Due to its higher content of valuable natural resources, its eco-toxicological and human health effects, mining house, government, non-governmental organization (NGO) and scientific communities are constantly exploring long-term and sustainable solution for the management, treatment, and valorisation of AMD. In addition, regulatory body required AMD to be treated and all pollutants reduced to acceptable level prior to its release into different environmental compartments; thus, implying an emergency action to be taken to effectively manage this unpleasant mine wastewater.

In line with that, preventive techniques such as drainage channels and limestone backfill around the mine site to hinder the AMD formation have been explored [9–11]. In addition to AMD formation prevention, various treatment technologies have been developed and are currently applied for the treatment of already generated AMD. They include active methods such as neutralization [12, 13], passive methods such as constructed wetland [2, 14–16], limestone bed [17–20], phytoremediation [21–23], hybrid and integrated technologies [24–26]. However, literature reports indicated some drawbacks associated with the above-mentioned treatment technologies; thus, limiting their application for effective treatment and valorisation of AMD. For instance, active technologies release highly polluted toxic sludge containing metals and other chemical species, which can be recovered using specific techniques. Passive methods are ineffective to treat highly acidic AMD water while hybrid and integrated technologies are fragile and require high capital cost [27]. Based on that, studies are been oriented on the treatment and valorisation of acid mine water and it is mostly accomplished by increasing the pH to desired level, collect and valorise sludge by recovering valuable minerals using various techniques including precipitation (neutralization) [1, 28], adsorption [29], ion-exchange [30], membrane technology [31], desalination [32] and bio-sorption [33].

However, valuable minerals recovery from AMD is complex at industrial level due to various drawbacks associated with each technique. For instance, membrane technology has the problem of membrane fouling, brine generation and high capital cost. Adsorption and ion-exchange are

ineffective to treat very acidic AMD water and are easily saturated. Desalination is not sustainable due to high capital and operational cost and the production of salt with impurities. Among those techniques, precipitation appears to be the most promising technology due to its ability to handle gigantic volume of AMD with very little dosage of alkaline chemicals, and the possibility to adjust it in step-wise fashion or selective precipitation to precipitate and recover chemical species at different pH gradients [1, 34]. On the other hand, bio-sorption is a physicochemical process that utilises the mechanism of absorption, adsorption, ion exchange and surface complexation to remove pollutants from aqueous solution [35, 36]. Furthermore, bio-sorption using agricultural by-products is cost effective, does not generate sludge and bio-adsorbent are readily available. Amongst the agricultural by-products, banana peels (BPs) is most suitable to remove chemical species (metals and sulphate) since its biomass contain functional group like carboxyl, hydroxyl and amine, which play a vital role for binding and remove pollutants from aqueous solution [37, 38].

As such, there is dire need to come up with innovative technologies that will exhibit the viability and feasibility of integrating fractional or sequential precipitation and bio-sorption for the treatment and valorisation of AMD and agricultural by-products in a circular economy approach (CEA) concept. Various techniques including electro reactions [39] and bio-electrochemical system [40] have been applied to recover valuable minerals from AMD while alkaline materials such as  $Ca(OH)_2$  and  $Na_2S$  [41], hydrated lime, soda ash and caustic soda [34],  $Na_2SO_4$  [42], and  $MgCO_3$  [1] have also been used to precipitate and recover valuable minerals from AMD. From literature, magnesium oxide (MgO) has high neutralisation capacity with optimum pH achievable of 9.5 and it has been successfully investigated for the active treatment of real AMD water [43–45], while BPs is effective bio-sorbent for chemical species removal in acid mine water, however, with limited efficiency in very acidic mine water [46, 47]. Owing to their disadvantages, which include the incapacity of MgO to increase the pH of AMD water above 9.5, and poor efficiency of BPs for concentrated acidic mine water, this complementary approach is being proposed to eliminate the drawbacks of each system to ensure the effective treatment and valorisation of AMD in order to control environmental pollution associated with both mining and agricultural activities. To the best of authors knowledge, the integration of fractional or sequential precipitation with MgO and bio-sorption using BPs has not been investigated for the treatment and valorization of AMD. Therefore, this is the first study in design and execution to explore the use of selective precipitation with MgO and bio-sorption with BPs for the treatment and valorization of real AMD. The proposed technique is cost effective, efficient, environmentally friendly and will open the route to introduce 4R (Recovery, reuse, recycle and repurpose) technology to valorize agricultural by-products, turn mining influenced water or AMD into beneficial products thereby controlling environmental pollution and reduce human health risks associated with exposure to contaminated waste.

## MATERIALS AND METHODS

### Reagents Acquisition and Standards Solution Preparation

Analytical grade and commercially produced MgO (99.99%) was purchased from Merck, South Africa while multi-element standard solution was purchased from Sigma-Aldrich, St Louis, Mo, USA). The calibration standard solutions were prepared using 100 mg/L multi-element (Sigma-Aldrich, St Louis, Mo, USA) for metals analysis while a sulphate standard solution (HACH, USA) of 1000 mg/L was used to prepare the calibration standards for  $\text{SO}_4^{2-}$  analysis. Ultrapure deionized water from a MilliQ Direct 8 water purifier system (Millipore S.A.S Molsheim, France) with resistivity of 18.1 M $\Omega$ /cm at 25 °C was used for the preparation of all standard solutions.

### Raw AMD Collection and Bio-sorbents (BPs) Acquisition

Raw AMD used in this study was collected from the discharge point of a coal mine in Limpopo province, South Africa. Acid mine water was collected using 5 L polyethylene container to prevent further oxidation and precipitation of metals. To obtain BPs which were used as bio-sorbent, ripe banana was purchased from a recognized franchised grocery store (Food Lover's Market), Johannesburg, South Africa. Once in the university laboratory, BPs were separated from banana, cut into small pieces, and cleaned using ultra-pure water to remove dirt, dried using an oven dryer and grinded to obtain a particle size of less than 100  $\mu\text{m}$ .

### Treatment and Valorization of Real AMD Water

This section is divided in 2 parts of which step 1 consists of selective precipitation and recovery of chemical species from real AMD, while step 2 focuses on the use of bio-sorbent (BPs) to polish the product water by bio-sorption technique.

### Selective Precipitation and Chemical Species Recovery Approach

To assess the effects of MgO on chemical species precipitation, an initial quantity of MgO and AMD were mixed in the ratio of 1:2000 (1 g/2000 mL or w/v ratio) and stirred at 800 rpm. The pH of the solution was gradually raised in stepwise fashion by cautiously increasing the MgO dosage and stirred at 800 rpm using an overhead stirrer to reach the desired pH (pH 4, pH 6, pH 8 and pH 9.5). At each desired pH, the solution was allowed to stand for 3 h followed by the decantation of supernatant water and the recovery of sludge following the method of Masindi et al. [1]. The supernatant water siphoned at each pH level was used for the next step of the precipitation process to reach the next desired pH, however with the increasing of MgO dosage, if after stirring for 60 min, the desired pH gradients was not reached. The pH of the solution was monitored using a pH meter. The different pH intervals for chemical species precipitation were pH (1.7–4), pH (4–6), pH (6–8) and pH (8–9.5) and at pH (4, 6, 8 and 9.5), processed AMD water samples were collected for chemical species analysis while sludge materials were recovered for different characterization studies. The experiment was optimized using one-factor-at-a-time (OFAAT) approach whereby the effects of precipitator (MgO) was duly explored.

### Bio-sorption Technique Using Banana Peels

Bio-sorption is a process of binding ions from aqueous solution in contact with functional group that are present on the surface of biomass [48]. To polish the product water using BPs, two parameters (contact time and bio-sorbent dosage) were investigated. To assess the effect of contact time, product water reclaimed at pH 9.5 was mixed with BPs at the ratio 1:100 mL (w/v or 1 g/100 mL). The mixture was stirred at 800 rpm and the effect of contact time was observed for 10, 30, 60, 90, 120, 150, 180, 210, 240 and 300 min. The mixture was then allowed to stand for 3 h followed by the recovery of supernatant water and filtration using 0.22  $\mu\text{m}$  pore size nylon syringe filter membrane prior to analysis for chemical species concentration, while raw and AMD reacted BPs were characterized using different characterization techniques. To assess the effect of bio-sorbent dosage, an amount of 0.1, 0.25, 0.5, 0.75, 1, 1.25 and 1.5 g was added into separate beakers containing 100 mL of pre-treated AMD each. The mixture was stirred at 800 rpm at the optimum contact time of 300 min after which the solution was allowed to stand for 3 h followed by filtration using 0.22  $\mu\text{m}$  pore size nylon syringe filter membrane and then analyzed for chemical species contents. The effect of pH was not evaluated since the quest was to mimic the system near real environmental conditions, and this comprise testing the system under ambient temperature and pH in order to understand the robustness of the system in a real environment where pH will not be evaluated or adjusted. Schematic representation of the hybrid and stepwise approach is shown in Figure 1.

### Samples Preparation and Analysis

Raw AMD and treated water samples recovered at different pH levels during selective precipitation process and after bio-sorption technique were filtered using a 0.22  $\mu\text{m}$  pore size nylon syringe filter membrane to remove particles and avoid absorption of metals [49], followed by the measurement of pH, EC and TDS. The water samples were then divided into two sub-samples of which sub-sample 1 was preserved by adding two drops of 65% nitric acid ( $\text{HNO}_3$ ) to avoid ageing and immediate precipitation of metals and kept at 4 °C until analysis for metals concentration using inductively coupled plasma optical-emission spectrometry (ICP-OES), 5110 ICP-OES vertical dual view, (Agilent technologies, Australia). Sub-sample 2 was left non-acidified and analyzed for  $\text{SO}_4^{2-}$  concentration using ion chromatography (IC) (850 professional IC Metrohm, Herisau, Switzerland). The two sub samples were analyzed following standard methods as stipulated by the American Public Health Association [50]. Sludge collected at different pH gradients were purified by drying at 125 °C for 24 H using dryer oven (Labotec Ltd, South Africa) while a grinder (Kambrook ASPIRE, South Africa) was used to mill the dried BPs to powder. After purification, 1 g of processed MgO was digested in a mixture of 6 mL of 37% hydrochloric acid (HCL) and 2 mL of 65% nitric acid ( $\text{HNO}_3$ ) using microwave digestion system (Anto Paar Strasse, Austria) as described by Uddin et al. [51], while the rest of purified sludge was used for different

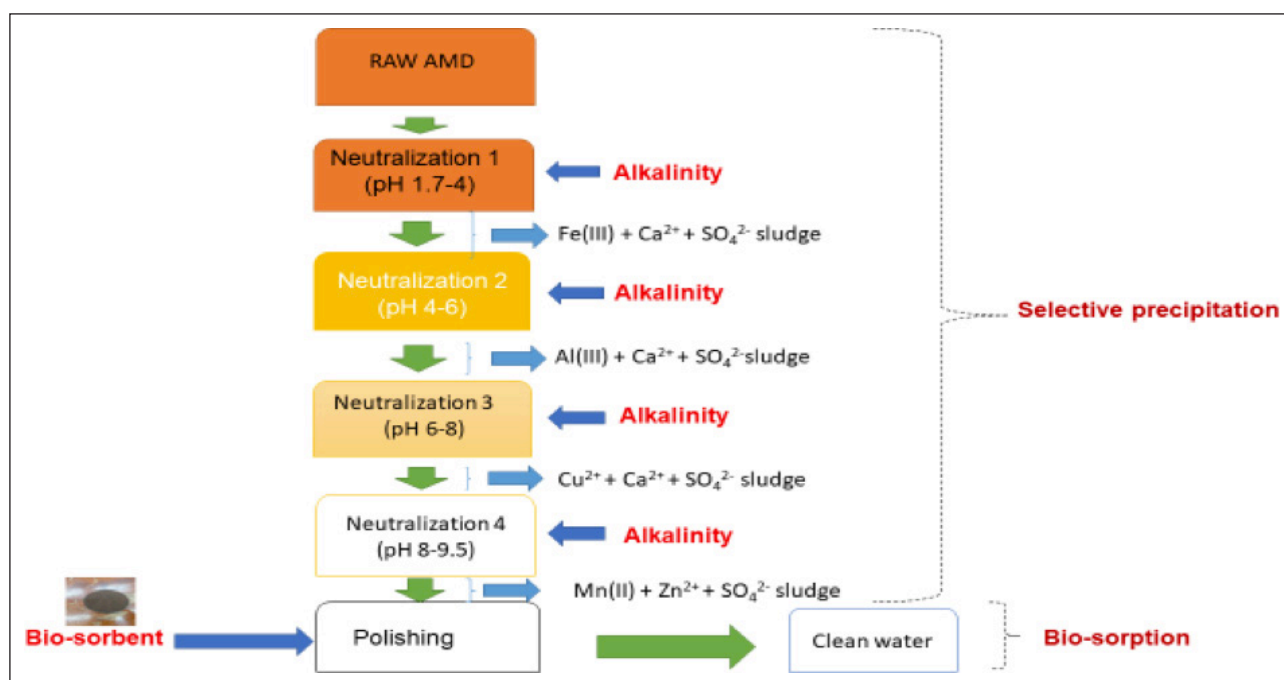


Figure 1. Schematic illustration of the hybrid system: selective precipitation and bio-sorption technique.

characterization studies. The digested samples were filtered using 0.22  $\mu\text{m}$  pore size nylon syringe filter membrane followed by analysis for chemical species concentration.

### Characterization Studies

Characterization studies were performed using different analytical and state-of-art characterization techniques. To be precise, morphological structures of pure, processed MgO, pure and BPs after treatment were determined using high resolution scanning electron microscopy energy dispersive x-ray spectroscopy (HR-SEM-EDS) (TESCAN VEGA 3 LMH Brno-kohoutovice, Czech Republic) coupled to an EDS (Oxford Instruments, Buckinghamshire, UK). The crystallographic structure and mineralogical composition were ascertained using powder X-ray diffraction (p-XRD) (Philips PW 1710, Netherlands) while different functional group were determined by Fourier transform infrared (FTIR) spectroscopy (Shimadzu, Kyoto, Japan) in the wavelength range between 500 and 4500  $\text{cm}^{-1}$  and scanned at a resolution of 16  $\text{cm}^{-1}$ . A PerkinElmer STA 6000 thermogravimetric analyser (TGA) (TA instruments, New Castle, USA) was used to determine the thermal stability of bio-sorbent and their fraction of components while a Malvern Zetasizer NANO-ZS ZEN3600 (Malvern panalytical, South Africa) was used to determine the particles in suspension on the surface of bio-sorbent.

### Regeneration of Banana Peels

A regeneration study was conducted for the BPs by mixing 0.5 g of bio-sorbent with a pre-treated AMD water collected at pH 9.5 with chemical species concentration as follows: Al (1.02 mg/L), Cu (0.01 mg/L), Fe (2.4 mg/L), Mn (1.03 mg/L), Ni (0.01 mg/L), Zn (0.09 mg/L) and  $\text{SO}_4^{2-}$ . The mixture was stirred at 800 rpm for a contact time of 300 min after which the bio-sorbent was recovered by filtration while the aqueous solution (pre-treated AMD) was analyzed for quantification

of chemical species concentration. The same procedure was repeated 5 times to evaluate the reusability of bio-sorbent.

### Quality Control and Quality Assurance

A quality control (QC) and quality assurance (QA) process was implemented in this study to warrant the production of trustworthy results. The QC/QA process required all analysis to be conducted in triplicate and data reported as mean value and considered acceptable when the difference between triplicate samples was less than 5% while the limit of detection (LOD) and limit of quantification (LOQ) were determined using standard methods.

### Limit of Detection and Limit of Quantification

To determine the LOD and LOQ, calibration curves with the following concentration of each element: 0.1, 0.3, 0.7, 1, 1.3, 1.5, 2, 2.5, 3 and 3.5 were used. A reagent blanks were analyzed to calculate the LOD. A standard solution containing about 10 mg/L of each element was used to obtain the standard intensities signal and the LOD was then calculated following the methods as illustrated in Equation (4) [52].

$$LOD = \frac{3 \times \sigma \times S}{I - \beta} \times V \quad (4)$$

Where:

$\sigma$  is the standard deviation of the blank solution

$S$  is the concentration of the standard (mg/L)

$I$  is the signal intensity of the standard

$\beta$  is the average intensity of the blank signal

$V$  is the volume of the final volume of the sample (9 mL).

The LOQ was then determined taking into account the fact that LOQ is approximately 3.333 times the LOD equation (5) [37].

$$LOQ = LOD \times 3.333 \quad (5)$$

**Table 1.** Raw AMD quality as compared to regulatory requirement

Parameters	Unit	Raw AMD	DWS guideline for drinking water quality	WHO guideline for drinking water quality	DEA guideline for effluent discharge
pH	–	1.7	5–9.8	6.5–8.5	6–12
EC	µS/cm	5000	150	≤400	0–700
TDS	mg/L	7380	1200	≤600	2400
Al	mg/L	160	≤0.3	0–0.1	20
Cu	mg/L	2.50	≤0.3	0–0.1	20
Fe	mg/L	6000	≤0.3	0–0.3	50
Mn	mg/L	40.7	≤0.1	0–0.08	20
Ni	mg/L	1.53	≤0.7	0–0.07	10
Zn	mg/L	8.00	≤0.5	0.0.1	20
SO <sub>4</sub> <sup>2-</sup>	mg/L	12500	≤500	≤250	2400

AMD: Acid mine drainage; DWS: Department of Water and Sanitation; DEA: Department of Environmental Affairs.

### Mathematical Modelling and Removal Efficiency

The efficiency of the hybrid approach (selective precipitation and bio-sorption) for the treatment and valorization of acid mine water was duly investigated. The removal efficiency (RE) was calculated for metals, EC, TDS and SO<sub>4</sub><sup>2-</sup> as demonstrated in equation (6) [14].

$$RE = \frac{C_i - C_f}{C_i} \quad (6)$$

Where C<sub>i</sub> and C<sub>f</sub> are the initial and final concentration of metals, respectively.

The pH increment was determined as illustrated in equation (7) [2].

$$I = pH_f - pH_i \quad (7)$$

Where pH<sub>f</sub> is the final pH of the product water, pH<sub>i</sub> is the initial pH of AMD, while I is the increment of pH after selective neutralization and bio-sorption.

The efficiency of selective precipitation using MgO and metals recovery was duly explored by determining the concentration of chemical species in sludge material and AMD water collected at each pH level followed by the calculation of the percentage of chemical species recovered at various stages of selective precipitation process as illustrated in equation (8) [53–57].

$$Recovery\ percentage\ (\%) = 100 \times \frac{C_p \times M_p}{C_{AMD} \times V_{AMD}} \quad (8)$$

C<sub>p</sub> is the concentration of the chemical species in the sludge material

M<sub>p</sub> is the mass of the sludge material

C<sub>AMD</sub> is the concentration of the chemical species in AMD water collected at each pH level

V<sub>AMD</sub> is the volume of AMD water at each pH gradients.

## RESULTS AND DISCUSSION

### Chemical Composition of Raw AMD

The chemical properties of AMD sample was determined using standard methods for water and wastewater [50] and

the results were compared to the South African regulatory bodies and World Health Organization (WHO) guidelines for drinking water and environmental discharge as presented in Table 1.

From Table 1, it follows that raw AMD collected was above national regulatory bodies, which include Department of Water and Sanitation (DWS) guidelines for drinking water, Department of Environmental Affairs (DEA) guidelines for effluent discharge and WHO water quality guidelines and therefore not suitable to be discharged untreated into different environmental compartments. The chemical composition revealed low pH, high EC and TDS, elevated concentration of major ions (Al, Fe, Mn and SO<sub>4</sub><sup>2-</sup>) and low concentration of trace elements (Cu, Ni and Zn). The elevated concentrations of Al, Fe and Mn indicate that these metals can be potentially recovered from AMD, while the recovery of trace metals (Cu, Ni and Zn) will be challenging due to their low concentrations. The elevated concentrations of Fe and SO<sub>4</sub><sup>2-</sup> indicate that AMD used in this study was formed following the oxidation of FeS<sub>2</sub> as reported in previous study [7].

### Percentage of Chemical Species Recovered

The percentage of chemical species recovered using selective precipitation under pH control was determined and the results are presented in Figure 2.

The Figure 2 depicted that Fe, Al, Mn, Zn and gypsum (CaSO<sub>4</sub>·2H<sub>2</sub>O) were the chemical species recovered throughout the pH range (1.7–9.5). At pH (1.7–4) interval, Fe(III) was the most recovered chemical species, followed by CaSO<sub>4</sub>·2H<sub>2</sub>O and Al. The recovery of Fe(III) at this pH interval was expected since Fe(III) is mostly precipitated at pH (2.5–4) interval in the form of Fe-hydroxide and Fe-oxy-hydrosulphates [1]. The small percentage of Al recovered at pH (1.7–4) interval may be credited to the presence of SO<sub>4</sub><sup>2-</sup> in AMD water. Typically, Al precipitates best at pH (4.5–7) [39]. However, the presence of SO<sub>4</sub><sup>2-</sup> slightly lowers the pH required for Al precipitation to less than 4 (pH ≤4)

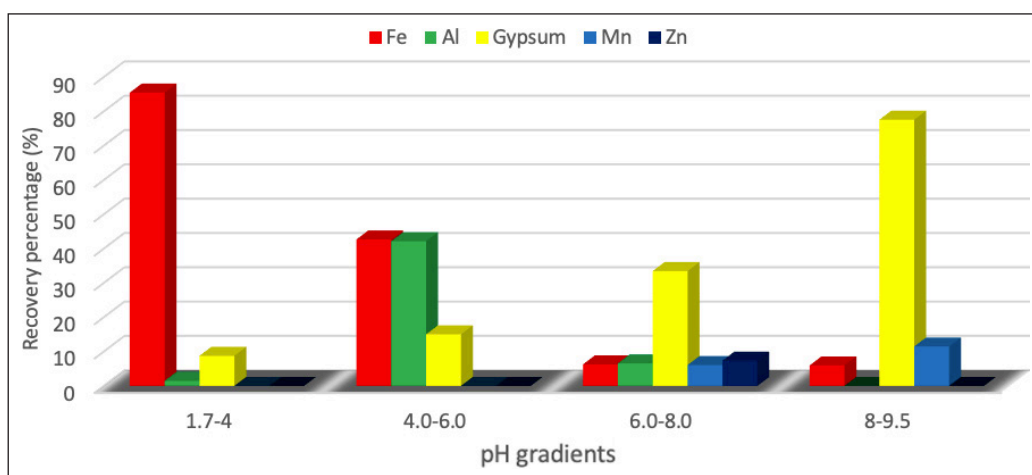


**Figure 2.** Recovery percentage of chemical species at four different pH intervals.

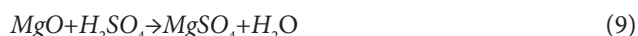
leading to the precipitation of minor quantity of Al at  $\text{pH} \leq 4$  and the formation of gibbsite  $[\text{Al}(\text{OH})_3]$  or Al-hydroxide as reported by previous studies [40, 41]. The recovery of  $\text{CaSO}_4 \cdot 2\text{H}_2\text{O}$  at this pH interval and throughout the pH range may be attributed to the precipitation of  $\text{Ca}^{2+}$  and  $\text{SO}_4^{2-}$ , which occurs at pH (2.5–11.5) interval [42, 43]. At pH (4–6) interval, Al and Fe were the most recovered chemical species and the quantity of Fe(III) recovered at this pH interval may be attributed to the continuous precipitation of  $\text{Fe}^{3+}$  from initial pH of 1.7 to 7.5 as reported by Seo et al. [34]. The recovery of high percentage of Al at this pH interval was expected since Al ion is mostly precipitated at  $\text{pH} \geq 4.5$ , while the continuous recovery of gypsum may be attributed to the continuous precipitation of  $\text{Ca}^{2+}$  and  $\text{SO}_4^{2-}$ , which start at  $\text{pH} \geq 2.5$ . At pH (6–8) interval, a minor percentage of Al and Fe was recovered and this may be attributed to the continuous precipitation of  $\text{Fe}^{3+}$  and  $\text{Al}^{3+}$  from pH 2.5 to pH of 7.5 and from  $\text{pH} \geq 4$ , respectively [34]. The findings in Figure 2, further revealed that a minor percentage of Mn was recovered at pH (6–8) interval and this may be attributed to the precipitation of Mn(II), which occurs at  $\text{pH} > 7$  to form Mn(II) hydroxide  $[\text{Mn}(\text{OH})_2]$  [58]. At pH (8–9.5) interval,  $\text{CaSO}_4 \cdot 2\text{H}_2\text{O}$  was the most recovered chemical species, while a moderate percentage of Mn in the form of  $\text{Mn}(\text{OH})_2$  was recovered at this pH interval. The recovery of  $\text{Mn}(\text{OH})_2$  may be attributed to the precipitation of  $\text{Mn}^{2+}$  while the high percentage of  $\text{CaSO}_4 \cdot 2\text{H}_2\text{O}$  is attributed to the precipitation of  $\text{Ca}^{2+}$  and  $\text{SO}_4^{2-}$ . Ideally,  $\text{Mn}^{2+}$  and  $\text{Mn}^{4+}$  are mostly precipitated at  $8 \geq \text{pH} \leq 9.5$  to form  $\text{MnO}_2$  and this may justify the percentage of Mn recovered at pH (8–9.5) interval. The recovery of a minor percentage of Fe may be attributed to the presence of ferrous ions under compound form, which precipitates at  $\text{pH} \geq 8$  to form ferrous hydroxide  $[\text{Fe}(\text{OH})_2]$  [59]. Overall, the chemical species recovered corroborated well with the EDS results.

#### Effect of Selective Precipitation and Bio-sorption on Water Quality of AMD

Raw AMD was treated using a combination of selective precipitation and bio-sorption techniques. Metals were gradually precipitated in raw AMD water using MgO, while BPs

were used to polish the product water by removing residual metals and  $\text{SO}_4^{2-}$  and the variation of the water quality is reported in Table 2.

As reported in Table 2, there was a significant increase of pH and reduction of chemical species concentrations with gradual or selective precipitation and bio-sorption techniques. Specifically, the selective precipitation and bio-sorption increased the pH from 1.7 to 10 corresponding to an increment of 8.3. The selective precipitation raised the pH from 1.7 to 9.5 which is the optimum pH level achievable using MgO while the bio-sorption by BPs bio-sorbent further raised the pH from 9.5 to 10. During the selective precipitation process using MgO, the mixture of MgO with AMD water stimulated the consumption of  $\text{H}^+$  from AMD water leading to the reduction of acidity and increase in pH as result of hydroxyl group ( $-\text{OH}$ ) by reaction with MgO [24, 60]. In fact, Once MgO is mixed with AMD, the reaction between MgO and  $\text{H}_2\text{SO}_4$  leads to the production of  $\text{MgSO}_4$  and water as illustrated in equation (9).



The continuous dissolution of MgO in acidic medium liberates magnesium ions ( $\text{Mg}^{2+}$ ) and hydroxide ions ( $\text{OH}^-$ ); thus, adding alkalinity in the solution and increasing of pH as shown in equation (10).



The bio-sorption step using BPs at 1:100 ratio (1 g:100 mL) (w/v) for a maximum contact time of 300 min allowed the binding of residual ions from aqueous solution via the adsorption mechanisms. In fact, BPs possesses various functional groups including hydroxyl group ( $-\text{OH}$ ), carbonyl ( $\text{C}=\text{O}$ ), amine group ( $-\text{NH}$ ) and unsaturated  $\text{C}=\text{C}$  group, which serve for binding ions from aqueous solution [61, 62]. These functional groups have adsorbed and removed residual chemical species from pre-treated AMD leading to complete removal of Al, Cu and Zn, and significant removal of other chemical species (Fe, Mn, Ni and  $\text{SO}_4^{2-}$ ). The removal of residual chemical species led to a slight increase of pH from 9.5 to 10. Overall, selective precipitation using MgO contributed to 94% of pH increment while

**Table 2.** Variation in AMD water quality as result of selective precipitation and bio-sorption

Parameters	Raw AMD	Selective or fractional precipitation				Bio-sorption
Volume (mL)	2000	2000	1870	1800	1720	1640
pH	1.7	4	6	8	9.5	10
MgO (g)	Nil	1	1.4	1.9	2.3	2.3 + 1g BPs
Al (mg/L)	160	141	2.30	1.79	1.02	<0.001
Cu (mg/L)	2.50	2.50	1.05	0.700	0.010	<0.002
Fe (mg/L)	6000	240	120	114	2.40	0.6
Mn (mg/L)	40.7	39.9	29.1	26.1	1.03	0.002
Ni (mg/L)	1.53	1.48	1.30	0.600	0.0100	0.001
Zn (mg/L)	8.00	7.72	3.21	2.30	0.0900	<0.005
SO <sub>4</sub> <sup>2-</sup> (mg/L)	12500	8400	6840	5400	3130	1250

AMD: Acid mine drainage.

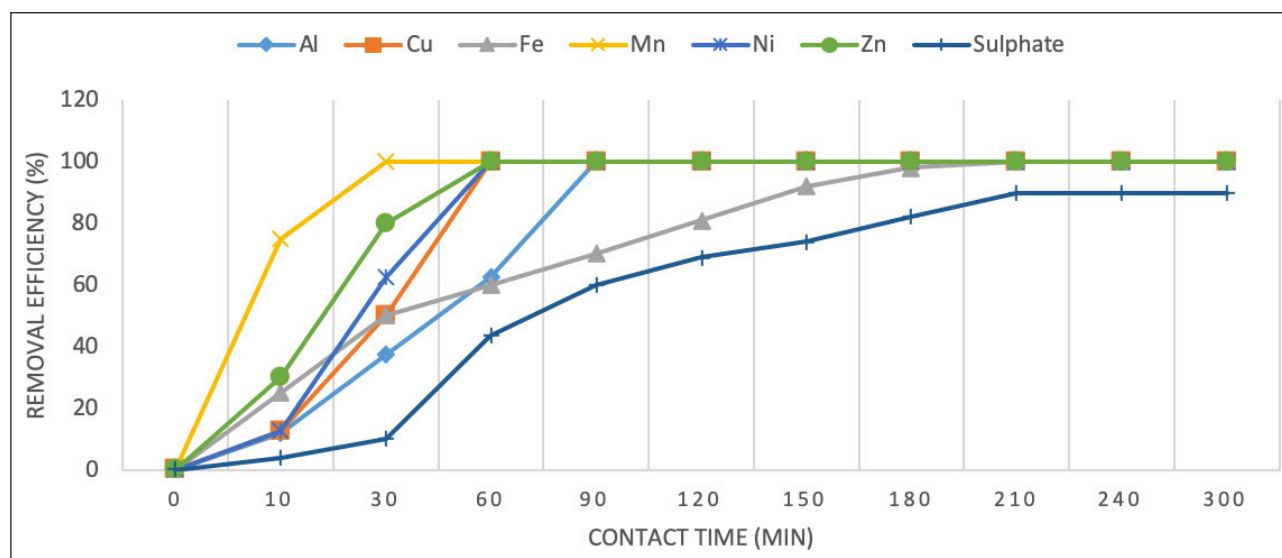


**Figure 3.** Effect of contact time on chemical species removal.

bio-sorption using BPs contributed to 6% of pH increment. The selective precipitation or step-wise precipitation process allows the pH to control the precipitation process and ensure the recovery of sludge rich in metals precipitated at different pH gradient as reported in the literature [1, 63]. The findings in Table 2 further revealed that pH 9.5 is the maximum pH level achievable using MgO for selective precipitation and neutralization. At the optimum pH level, chemical species were removed as follows: Fe (99.96%) > Cu (99.6%) > Al (99.36%) > Ni (99.34%) > Zn (99%) > Mn (97.47%) > SO<sub>4</sub><sup>2-</sup> (75%). The results were in line with previous studies [1, 28, 43], thereby confirming that selective precipitation using MgO is efficient to significantly attenuate and recover chemical species in AMD. The bio-sorption step using BPs further rose the AMD pH from 9.5 to 10 leading to more chemical species attenuation and at pH 10, the RE was very high (99.99%, 99.93%, 99.98% and 90%) for Fe, Ni, Mn and SO<sub>4</sub><sup>2-</sup>, respectively while Al, Cu and Zn were below the LOD of 0.001, 0.002 and 0.005 mg/L, respectively. Overall, the combination of selective precip-

itation and bio-sorption techniques allowed to precipitate different metals at different pH and reclaim water that meet the DEA guidelines for effluent discharge; however, should be further treated to reclaim drinking water standard since Fe and SO<sub>4</sub><sup>2-</sup> concentrations were above maximum permissible levels (MPLs) as set by WHO and the DWS in the Republic of South Africa (RSA). This hybrid system can serve as the bottom line to implement CEA concept to control environmental pollution associated with mining activities and agricultural industry.

In order to polish the product water obtained after selective precipitation technique, two parameters (effect of contact time and effect of adsorbent dosage) were evaluated.

**Effect of contact time on the adsorption of chemical species by BPs**

The effect of contact time in the bio-sorption step was assessed for chemical species of concern and the results are shown in Figure 3.

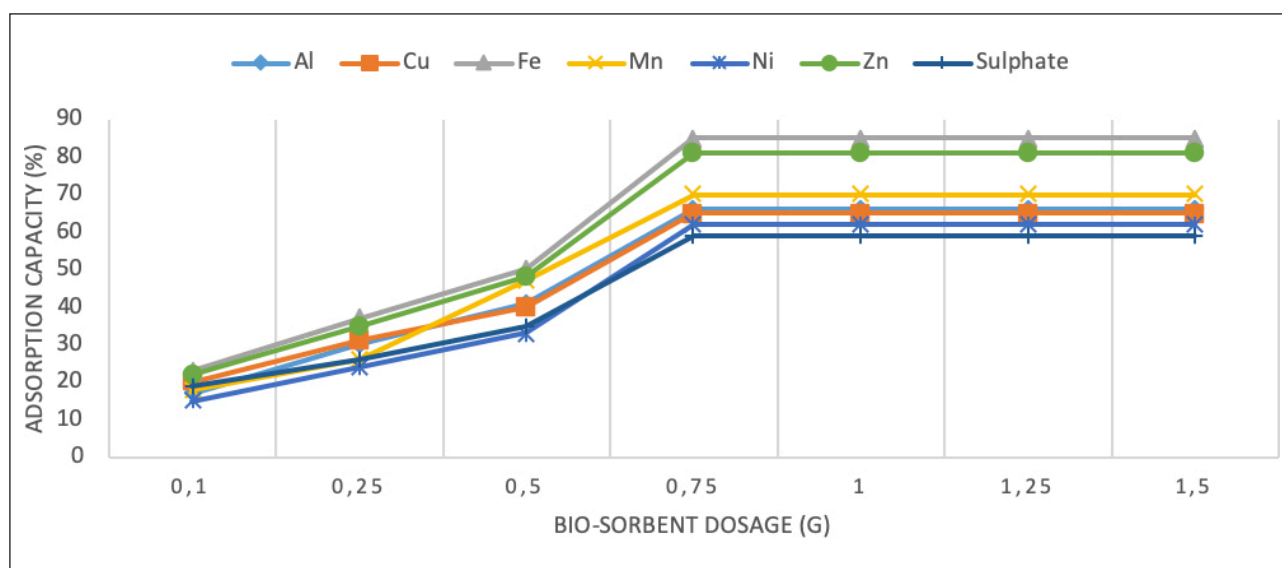


**Figure 4.** Effect of bio-sorbent (BPs) dosage on chemical species removal.

As shown in Figure 3, the contact time had a positive effect on chemical species adsorption since the RE of all chemical species increased as the contact time increased, however with different patterns. The significant increase in RE observed during the first 30 min may be attributed to the accessibility of active sites on the surface of bio-sorbent (BPs). However, the optimum contact differs for chemical species with 30 min being the optimum contact time for Mn, 60 min for Cu, Ni and Zn, 90 min for Al and 210 min for Fe and  $\text{SO}_4^{2-}$ . The difference in the optimum contact time may be attributed to the competition between chemical species to occupy available active sites on the surface of the bio-sorbent (BPs). According to Drew and Andrea [64], the competition process firstly involves cations competing with hydrogen ion ( $\text{H}^+$ ) to bind to oxide or carboxyl site and on the other hand, involve anions and cations competing to bind amine group. The difference in the optimum contact time may also be credited to the initial content of chemical species in pre-treated AMD used in the bio-sorption step since chemical species (Al, Cu and Zn) with very low concentration were completely adsorbed, Mn and Ni were nearly complete adsorption, while Fe and  $\text{SO}_4^{2-}$  were partially adsorbed. The complete adsorption of Al, Cu and Zn may be attributed to their very low concentrations after selective precipitation. However, the complete adsorption did not apply to Mn and Ni and this may be the result of competition process [64]. The partial adsorption of Fe and  $\text{SO}_4^{2-}$  may be attributed to the threshold limit of contact time or saturation of active sites after which the prolonged contact does not have any effect in adsorption capacity of bio-sorbent (BPs) and this can be due to slow diffusion of solute into the interior of bio-sorbent [65, 66]. The partial adsorption of Fe and  $\text{SO}_4^{2-}$  may also be credited to the saturation of active sites on the surface of bio-sorbent since after 210 min, the prolonged contact does not have any effect on the adsorption of Fe and  $\text{SO}_4^{2-}$  thereby confirming the results obtained in previous studies [67, 68].

#### Effect of BPs Dosage on the Removal of Chemical Species

The bio-sorbent dosage was investigated for the pre-treated AMD water reclaimed at pH 9.5. The dosage of BPs was varied in the following order: 0.1, 0.25, 0.5, 0.75, 1, 1.25 and 1.5 g and the results are shown in Figure 4.

The Figure 4 clearly depicted that the increase of bio-sorbent dosage led to an increase of RE and this can be credited to the large number of active sites resulting from the increase of bio-sorbent dosage, which provide large surface areas to adsorb chemical species [69]. The increase of active sites is the result of number of oxygen bearing functional groups including alcohols, carboxylic acids and esters as revealed by FTIR spectroscopy analysis of BPs. The Figure 4 further indicates that all chemical species were gradually adsorbed, and the saturation was reached with 0.75 g of bio-sorbent dosage, however at different RE in the following order: Fe (85%) > Zn (81%) > Mn (70%) > Al (66%) > Cu (65%) > Ni (62%) >  $\text{SO}_4^{2-}$  (59%). The variation in RE may be attributed to many factors, which include initial chemical species concentration, metals affinity to bio-sorbent, competing or co-existing ions and speed of agitation [70, 71]. The highest RE of Fe may be attributed to the facility of positively-charged metal to bind with an electron-rich hydroxyl group thereby confirming previous studies [72]. Overall, the effects of bio-sorbent dosage revealed two phases: phase 1 which is illustrated by a significant increase of RE from 0.1 g to 0.75 g and phase 2 which is illustrated by a constant RE from 0.75 g to 1.5 g and this can be credited to the availability of active sites during the phase 1 and the saturation of active sites during the phase 2 and the continuous addition of bio-sorbent does not have any effect on bio-sorbent capacity to adsorb chemical species. These results are in line with reports from previous studies [47]. This study proved that BPs have a great potential in chemical species removal and can be further investigated for polishing of pre-treated AMD.



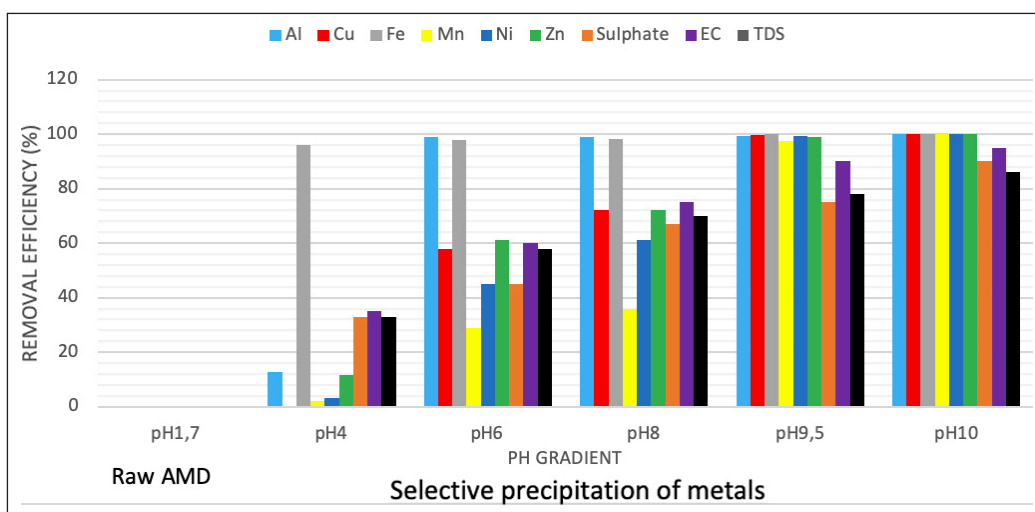


Figure 5. Variation in the percentage removal of chemical species as function of selective precipitation and bio-sorption.

### Removal Efficiency of the Hybrid System (Selective Precipitation and Bio-sorption) on AMD Quality Improvement

The RE of the hybrid system (selective precipitation and bio-sorption) was gradually evaluated and the results are shown in Figure 5.

Figure 5 clearly portrayed that the RE increased gradually as results of selective precipitation and bio-sorption techniques. This allowed to raise the pH from 1.7 to 10, complete removal of Al, Cu and Zn and other chemical species as follows: Fe (99.99%) = Mn (99.99%) > Ni (99.93%) > EC (95%) > SO<sub>4</sub><sup>2-</sup> (90%) > TDS (86%) proving that metals can be recovered, and possible drinking water standard reclaimed using a combination of selective precipitation and bio-sorption techniques. In particular, the selective precipitation using MgO allowed to precipitate metals at different pH gradients, rose the pH from 1.7 to 9.5. The increase of pH may be credited to the dissolution of MgO in the presence of water to liberate Mg<sup>2+</sup> ion and hydroxide ion (OH<sup>-</sup>), which react to form magnesium hydroxide [Mg(OH)<sub>2</sub>] as illustrated in the following equation (11) and (12).



The reactions add alkalinity in AMD thereby leading to pH increase, metals precipitation at different pH gradient and possible recovery. Selective precipitation reduced the concentration of chemical species with RE as follows: Cu (99.7%) > Fe (99.96%) > Al (99.36%) > Ni (99.34%) > Zn (99%) > Mn (97.47%) > SO<sub>4</sub><sup>2-</sup> (75%), while the bio-sorption technique further increased the pH from 9.5 to 10 and accounted for a minor fraction of chemical species removal with RE in the following order: SO<sub>4</sub><sup>2-</sup> (15%) > TDS (8%) > EC (5%) > Mn (2.53%) > Zn (1%) > Ni (0.66%) > Al (0.64%) > Cu (0.4%) > Fe (0.03%). The adsorption of chemical species using BPs led to more reduction of metals in aqueous solution and consequently reduction of H<sup>+</sup> resulting to slight pH increase from 9.5 to 10. However, Fe, Mn, Ni, EC, SO<sub>4</sub><sup>2-</sup> and TDS were not completely removed after treatment of mine water using se-

lective precipitation and bio-sorption technique and the percentage of not removed were 0.01%, 0.01%, 0.07%, 5%, 10% and 14% for Fe, Mn, Ni, EC, SO<sub>4</sub><sup>2-</sup> and TDS, respectively. This combination of selective precipitation and bio-sorption techniques yielded the best result for AMD treatment and valorization. Overall, the chemical treatment step contributed close to 97% of overall pollutants removal, while the bio-sorption step contributed only to 3% of overall chemical species attenuation; thus, designating it as a polishing stage.

### Overall Water Quality

Chemical properties of AMD before and after treatment using a combination of selective precipitation with MgO and bio-sorption using BPs were compared with guideline values for drinking water and effluent discharge as set by regulatory bodies and the results are presented in Table 3.

The parameters of concern were pH, TDS, EC and metals (Al, Cu, Fe, Mn, Ni, Zn) and sulphate ions. After the treatment using the hybrid technology, the pH of raw AMD rose from 1.7 to 10 leading to mostly complete removal of all metals of concerns except Fe and significant reduction of SO<sub>4</sub><sup>2-</sup>, EC and TDS. The findings corroborated with previous studies as revealed in the literature for both chemical treatment and biological treatment. In fact, selective precipitation allowed to significantly reduce metals and SO<sub>4</sub><sup>2-</sup> concentration, which can further be recovered [1, 43], while the biological treatment using BPs served as polishing step to remove residual chemical pollutants [47, 73]. The values of all chemical parameters of concern were within the DEA guidelines standard for effluent discharge. However, drinking water standard as set by WHO and the DWS in the republic of South Africa could not be directly reclaimed using this hybrid technology due to the high concentration of SO<sub>4</sub><sup>2-</sup> (1250 mg/L) and Fe (0.6 mg/L) in final product water which are slightly above the MPLs of 500 mg/L and 0.1 mg/L for SO<sub>4</sub><sup>2-</sup> and Fe, respectively. Nevertheless, the finding of this study revealed that valuable minerals (Al, Fe, Mn, and gypsum) could be recovered from AMD using selective precipitation due to their high concentrations in raw

**Table 3.** Concentration of chemical species in AMD water before and after treatment compared to DEA, DWS and WHO

Parameters of concern	Raw AMD	Treated AMD	Removal efficiency (%)	DWS guidelines for drinking water	WHO guidelines for drinking water	DEA guidelines for effluent discharge
pH	1.7	10	8.3 (increment)	5.5–9.7	6.5–8.5	6–12
EC ( $\mu\text{S}/\text{cm}$ )	5000	50	95	170	<400	700
TDS (mg/L)	7380	1030	86	2400	<600	1200
Al (mg/L)	160	<0.001	100	0–0.3	0–0.1	20
Cu (mg/L)	2.50	<0.002	100	0.1	0.1	20
Fe (mg/L)	6000	0.6	99.99	0–0.1	0–0.03	50
Mn (mg/L)	40.7	0.002	99.99	0–0.05	0–0.08	20
Ni (mg/L)	1.53	0.001	99.93	0–0.07	0–0.07	10
Zn (mg/L)	8.16	<0.005	100	0–0.05	0–0.1	20
$\text{SO}_4^{2-}$ (mg/L)	12500	1250	90	0–500	0–250	2400

AMD: Acid mine drainage; DWS: Department of Water and Sanitation; WHO: World Health Organization; DEA: Department of Environmental Affairs.

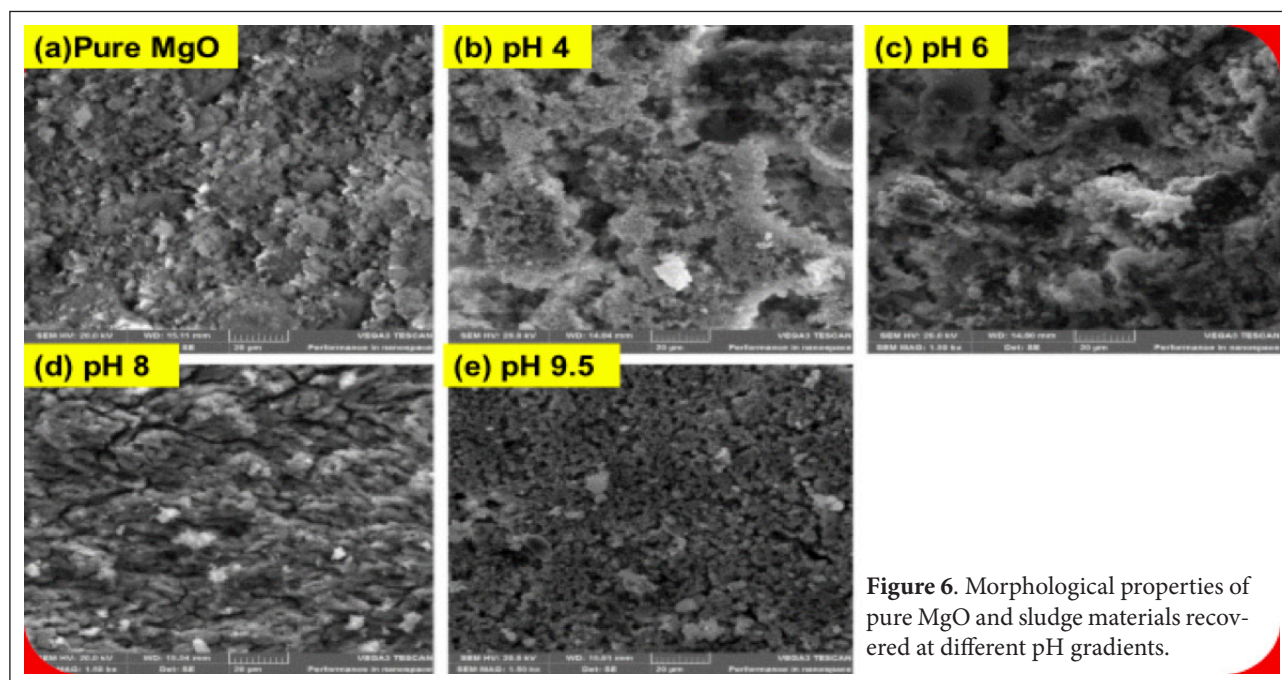


**Figure 6.** Morphological properties of pure MgO and sludge materials recovered at different pH gradients.

AMD water. However, Cu, Ni and Zn cannot be recovered due to the very low (trace) concentrations in raw AMD and as such, economically insignificant.

#### Characterization of the Solid Samples

In this section, the results of mineralogical composition, chemical composition, elemental spectra, functional group of raw MgO and sludge materials recovered at each pH interval raw and AMD treated with BPs as well as the mass change in BPs samples are discussed.

#### Morphological Properties of Raw MgO, Sludge and Banana Peels

##### Morphology Property of MgO and Sludge

Scanning electron microscopy analysis was performed to determine the morphological properties of pure MgO and

sludge materials recovered at each pH interval and the results are shown in Figure 6a–e.

The SEM image of raw MgO (Fig. 6a) revealed flower-like and shaped particles of two different size on the surface indicating that the material is heterogeneous in nature and characterized by two different elements proving that this material is MgO as revealed by EDS results. The finding is in line with what have been reported in literature [74]. Figure 6b, which represents SEM image of sludge material collected at pH 4 showed sheet-like structure across the surface indicating that the material is heterogeneous. The sheet-like structure may be attributed to iron hydroxide  $[\text{Fe}(\text{OH})_3]$  formed as results of Fe(III) precipitation. Similar results were obtained in previous studies [1, 43] proving that Fe(III) was effectively precipitated at  $\text{pH} \leq 4$  to form  $\text{Fe}(\text{OH})_3$  and Fe-oxyhydrosulphates. At pH 4 (Fig. 6c), the

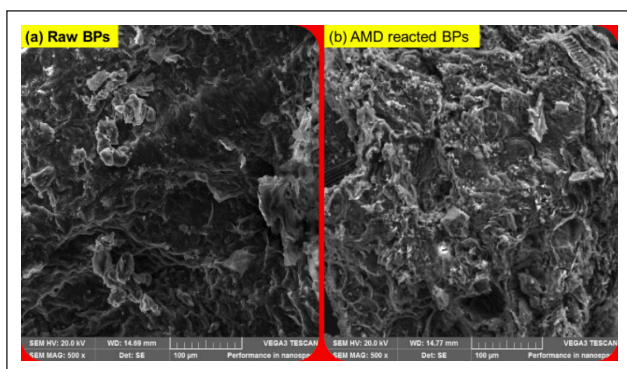


**Figure 7.** Morphological properties of raw and AMD treated with banana peels.

SEM images of sludge materials showed a sort of foliage like and unshaped structures assembled to give the whole materials an irregular structures and may indicate the presence of  $\text{Al}(\text{OH})_3$  in elevated concentration and minor concentration of  $\text{Fe}(\text{OH})_2$ . This is a prove that Al were effectively precipitated from  $\text{pH} \geq 4.5$  [75]. The result corroborated with reports from previous studies [41]. At  $\text{pH} 8$  (Fig. 6d), the SEM image of sludge materials showed an assemblage of cylindrical form clustered together to form a homogeneous structure across the whole surface. This is an indication of many chemical species precipitated including Cu which is precipitated at  $\text{pH} > 6$  [56, 57] and  $\text{Ca}^{2+}$  and  $\text{SO}_4^{2-}$  which are precipitated throughout the  $\text{pH} (2.5-9.5)$  range to form  $\text{CaSO}_4 \cdot 2\text{H}_2\text{O}$ . At  $\text{pH} 9.5$  (Fig. 6e), the SEM images of sludge materials collected showed a heterogeneous structure across the whole surface with large smooth surface, which may be attributed to the formation of  $\text{Mn}(\text{OH})_2$  followed the precipitation of  $\text{Mn}(\text{II})$  and  $\text{Mn}(\text{IV})$  suggesting that major chemical species susceptible to be recovered at  $\text{pH} (8-9.5)$  is Mn since it is precipitated at the  $\text{pH} 8-9.5$  interval [76]. The presence of bright materials on the surface may represent silicon as confirmed by EDS results while the presence of round shapes may represent the formation of  $\text{Fe}(\text{OH})_2$  following the precipitation of  $\text{Fe}(\text{II})$ .

**Morphological Properties of Banana Peels**

The SEM analysis of raw and AMD treated with BPs were performed, and the results are shown in Figure 7a, b.

The SEM micrograph of raw BPs and AMD treated with BPs showed different structure with raw BPs showing a smooth surface and various pores with fibers stacked together (Fig. 7a). This may be attributed to the presence of lignin, pectin and other bioactive compounds including phenolic, carotenoids, biogenic, amines and phytosterols [46]. After contact with AMD, the surface of BPs became less smooth with cave pores filled with a mass, which may represent residual chemical species adsorbed from AMD. The findings of this study confirmed what was reported in literature by other researchers when using BPs for metals removal in aqueous solution [77]. Overall, the SEM image of BPs results revealed that BPs contain organic compounds including cellulose that can absorb chemical species by allowing the ions of metals to be bonded by electron-rich functional group.

**EDS Results of Pure MgO, Sludge Materials and Banana Peels**

**EDS Results of Pure MgO and Sludge Recovered at Different pH Gradients**

The effect of selective precipitation process and pH control on metals recovery was gradually assessed using elemental distribution of minerals at each pH gradient and the results are shown in Figure 8a–e.

As shown in Figure 8a (pure MgO), EDS of raw MgO revealed that only two elements were present (Mg and O) with Mg as major element and O being a minor element. Magnesium is alkaline chemical with high chemical reactivity and contribute to increase the alkalinity when mixing with water [78, 79]. This makes MgO a suitable candidate for selective precipitation and metals recovery from AMD under pH control. At  $\text{pH} 4$  (Fig. 8b), the EDS of sludge collected revealed that O, Mg and Fe as major components, moderate percentage of sulphur (S), minor percentages of Al, Ca and Mg, and  $\text{SO}_4^{2-}$  and finally trace amounts of Si. The high percentage of O is attributed to the oxygen from MgO and from water molecule while the elevated percentage of Fe is attributed to the precipitation of  $\text{Fe}(\text{III})$  from AMD leading to the formation of complexed iron hydroxides [ $\text{Fe}(\text{OH})_3$ ] and subsequently solid precipitates since  $\text{Fe}(\text{III})$  is mostly precipitated in the  $\text{pH} \leq 4$  [80]. The moderate percentages of S and minor percentage of Al suggest that there is possibility of Fe-oxyhydrosulphates and aluminum hydroxide [ $\text{Al}(\text{OH})_3$ ] being formed at  $\text{pH} 3-4$  as revealed by previous studies [80]. The minor percentage of Al obtained from sludge materials recovered at this  $\text{pH} \leq 4$  may also be attributed to the slight precipitation of Al due to the presence of  $\text{SO}_4^{2-}$  thereby confirming the findings reported in previous studies where a minor proportion of Al is precipitated at  $\text{pH} \leq 4$  [54, 80].

At  $\text{pH} 6$  (Fig. 8c), the recovered sludge material contains very high percentage of O, elevated percentage of Fe and Al. While the elevated percentage of Al is attributed to precipitation of  $\text{Al}^{3+}$  mostly occurs at  $\text{pH} \geq 4$  [34, 75], the elevated percentage of Fe is the result of continuous precipitation of  $\text{Fe}(\text{III})$ . The presence of S and Ca as minor component in the sludge material collected at  $\text{pH} 6$  indicates the continuous precipitation of Ca and  $\text{SO}_4^{2-}$  and possible formation of  $\text{CaSO}_4 \cdot 2\text{H}_2\text{O}$  as reported in literature [1, 34, 53]. The EDS further revealed moderate percentage of Al and Fe, minor percentage of Ca, Mn, S, Si and Zn and trace amount of Cu, K and Y. At  $\text{pH} 9.5$ , the sludge material recovered revealed high percentage of Ca, Minor percentage of Mn, S and Fe and trace of Si, Cu and Na. The high percentage of Ca is attributed to the precipitation of Ca which reach the peak at  $\text{pH} 8.5$  while the presence of minor narrow percentage of Fe may be credited to presence of  $\text{Fe}(\text{II})$ , which precipitate at  $\text{pH} \geq 8$  to form  $\text{Fe}(\text{OH})_2$  [59]. In addition,  $\text{Fe}^{3+}$  is precipitated from initial pH to  $\text{pH} 7.5$  [34] and this can explain the presence of  $\text{Fe}(\text{III})$  in sludge material recovered at  $\text{pH} \geq 4$  thereby overlapping with Al at the precipitation pH interval since both Fe and Al are present in sludge materials recovered throughout the  $\text{pH} 4-8$  interval. The presence

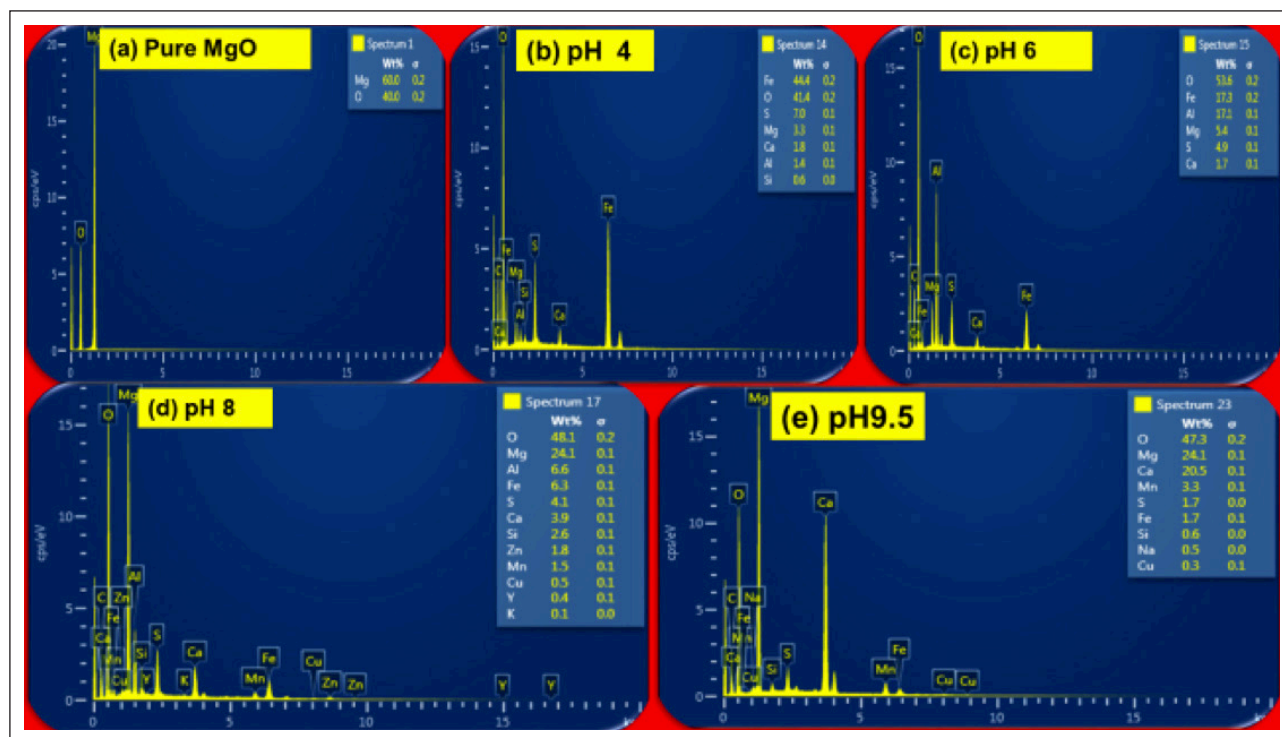


**Figure 8.** Energy dispersive X-ray spectroscopy results of pure MgO and sludge materials recovered at different pH gradients.

of Fe and Al in sludge materials recovered throughout the pH interval may also be attributed to the co-precipitation of Fe(III) and Al. In fact, Fe(II) precipitates at pH (8–9.5), while Al precipitates at pH  $\geq 4.5$  and this may justify the presence of Fe and Al in sludge materials recovered thereby confirming previous studies [80]. The presence of Al and S at pH 4–8 interval suggests the formation of Al-hydroxide and Al-oxhydroxysulphates, respectively thereby confirming the findings of studies conducted by previous researchers [80–82]. The presence of Mn indicates the precipitation of Mn(II) and Mn(IV) which occurs at pH  $\geq 8$  since EDS results of this study revealed the presence of Mn in sludge materials recovered at pH 8–9.5 interval. The results were in line with previous studies conducted by Masindi et al. [1] when they used cryptocrystalline magnesite for a selective precipitation of metals in AMD water. Due to its many oxidation states, Mn(II) and Mn(IV) precipitate at variable pH range ( $8 \leq \text{pH} \leq 10$ ) and this justify the high percentage of Mn in sludge material recovered at pH (8–9.5) interval [83].

#### **EDS Results of Raw and Treated with Banana Peels**

The product water reclaimed at pH 9.5 was further polished by means of bio-sorption techniques using BPs to remove residual chemical species and reclaim possible drinking water standard. The spectra of raw and AMD treated with BPs are shown in Figure 9a, b.

As illustrated in Figure 9a, the EDS of raw BPs revealed the presence of various elements along with O, K, Si and Ca as major components with percentage composition of 77.1%, 9.5%, 6.4% and 3.2%, respectively while P, Mg, S and Cl with percentage composition of 1%, 1%, 0.9% and 0.9%, respectively are trace components. The high levels of O, K, Si and

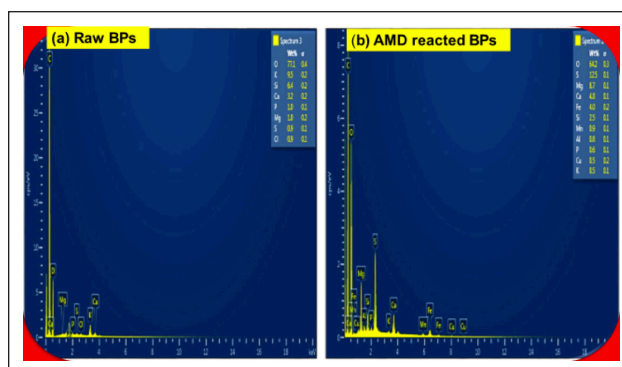


**Figure 9.** Energy dispersive X-ray spectroscopy of raw and AMD treated with banana peels.

Ca in raw BPs confirmed the heterogeneous structure of BPs bio-sorbent as reported in the literature [83–85]. This may be attributed to chemical composition and different functional groups present in BPs bio-sorbent. After contact with AMD water (Fig. 9b), the BPs revealed the presence of more elements of which O and Mg, were major components with a percentage of 45.7% each, Ca, S and Mn were minor elements with a percentage composition of 3.7%, 2% and 1.2%, respectively while Fe, Al Si, K and Cl were trace elements with a percentage composition of 0.5%, 0.4%, 0.4% 0.2% and 0.1%, respectively. The presence of S, Fe, Ca, Al and Mn, in AMD treated with BPs is attributed to its use as bio-sorbent to polish the AMD water previously treated using selective precipitation technique; thus, confirming that their removal from AMD. The EDS results proved that BPs adsorbed residual chemical species, thereby confirming the results obtained after analysis of final product water.

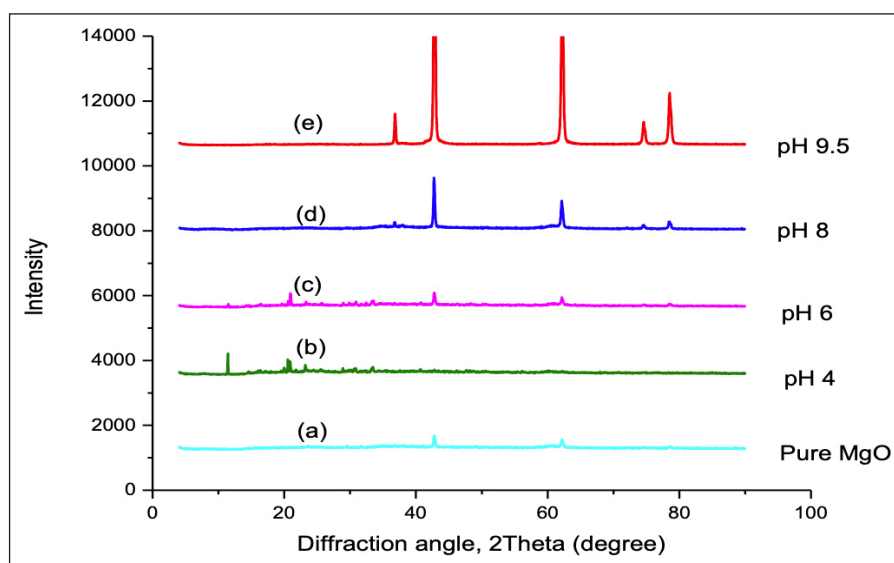


**Figure 10.** Powder X-ray diffraction results of pure MgO and sludge materials recovered at different pH interval: pH 4, pH 6, pH 8 and pH 9.5.

**Powder X-ray Diffraction Results of Pure MgO Sludge Materials And Bio-sorbent**

**Powder X-ray Diffraction of Pure MgO and Sludge Materials**

The sludge materials recovered at different pH levels were analyzed for chemical phase present and chemical composition information and the results are shown in Figure 10a–e.

From Figure 10, it follows that raw MgO is almost amorphous showing two peaks at  $2\theta = 43^\circ$  and  $2\theta = 62^\circ$  likely revealing the presence of polycrystalline cubic structure of MgO [86]. These peaks may correspond to periclase which is the only crystalline form of MgO as revealed by previous studies [86]. However, after using MgO for selective precipitation of metals in AMD water, the pH of AMD water rose from 1.7 to 4. The sludge material recovered at pH 4 interval showed a series of peaks at  $2\theta = 11^\circ, 20^\circ, 22^\circ, 29^\circ$  and  $35^\circ$ . These peaks may correspond to Fe-hydroxide formed at pH 3.5–4 thereby confirming SEM-EDS results, proving that Fe can be recovered from sludge materials recuperated at pH 4. Similar p-XRD results were obtained by previous researchers [1, 28, 43] where they used different chemical materials for metals recovery from AMD. At pH 6, the sludge materials recovered showed peaks at  $2\theta = 20^\circ, 34^\circ, 40^\circ$  and  $62^\circ$ , which may indicate the presence of Al, calcite and gypsum. At pH 8 interval, p-XRD analysis revealed peaks at  $2\theta = 43^\circ, 62^\circ, 75^\circ$  and  $79^\circ$ , which may indicate the presence of gypsum resulting from  $\text{SO}_4^{2-}$  precipitation at  $\text{pH} \geq 4.5$  as revealed by previous studies [56]. At pH 9.5 interval, the sludge materials collected showed various peaks with peak at  $2\theta = 36^\circ$ , which may indicate the presence of Mn. The peaks at  $2\theta = 43^\circ$  and  $62^\circ$  indicate the presence of brucite, while the peaks at  $2\theta = 75^\circ$  may correspond to copper(II) oxide (CuO) formed following the precipitation of Cu at  $\text{pH} > 6$  and the peak at  $2\theta = 79^\circ$  may indicate the nickel oxide (NiO) following the precipitation of nickel at pH 8–9 interval [87]. The difference in intensity may be explained by the fact that as intensity increases, the diffraction process becomes narrower and more intense.

**Powder X-ray Diffraction Results of BPs Bio-sorbent**

The product water reclaimed at pH 9.5 was polished using BPs and the p-XRD analysis results are shown in Figure 11a, b.

The p-XRD analysis of raw BPs (Fig. 11a) and AMD treated with BPs (Fig. 11b) revealed a typical cellulose structure at  $2\theta = 14^\circ$  for raw BPs and  $2\theta = 20^\circ$  for AMD treated with BPs [88, 89]. The series at  $2\theta = 30^\circ, 34^\circ, 37^\circ, 40^\circ$  and  $52^\circ$  in AMD treated with BPs is the evidence of the presence of chemical species notably Al, Cu, Fe, Mn and  $\text{SO}_4^{2-}$  as revealed by EDS results thereby confirming what has been reported in literature [47]. Based on the p-XRD results, it can be concluded that BPs adsorbed residual chemical species from pre-treated AMD.

**Fourier Transform Infrared (FTIR) Spectra of Sludge and BPs**

**FTIR Spectra of Pure MgO and Sludge Materials**

The functional groups of pure MgO and sludge collected at different pH levels were analyzed and the results are shown in Figure 12a–e.

Figure 12 portrayed that raw MgO is characterized by the vibration at  $500\text{ cm}^{-1}$ , which may be attributed to carbonate species chemisorbed on the surface of MgO as reported by previous researchers [90]. The FTIR spectra of pure MgO and all sludge materials recovered at different pH levels showed the doublets at  $2000$  and  $2150\text{ cm}^{-1}$ , which may be attributed to the Mg-O stretching vibration [90], while the stretching vibration at  $2600\text{ cm}^{-1}$  in pure MgO may correspond to asymmetric stretching vibration of alkyl (C-H) functional group [90, 91]. The sludge materials recovered at pH 4, pH 6, pH 8 and pH 9.5, intervals showed peaks with stretching vibration at  $1100\text{ cm}^{-1}$ , which may be attributed to carbonate esters functional group  $[\text{R}_1\text{O}(\text{C}=\text{O})-\text{OR}_2]$  from AMD water as confirmed by SEM-EDS analysis, while the vibration at  $1670\text{ cm}^{-1}$  may correspond to hydroxyl functional group (O-H) or carboxyl function-

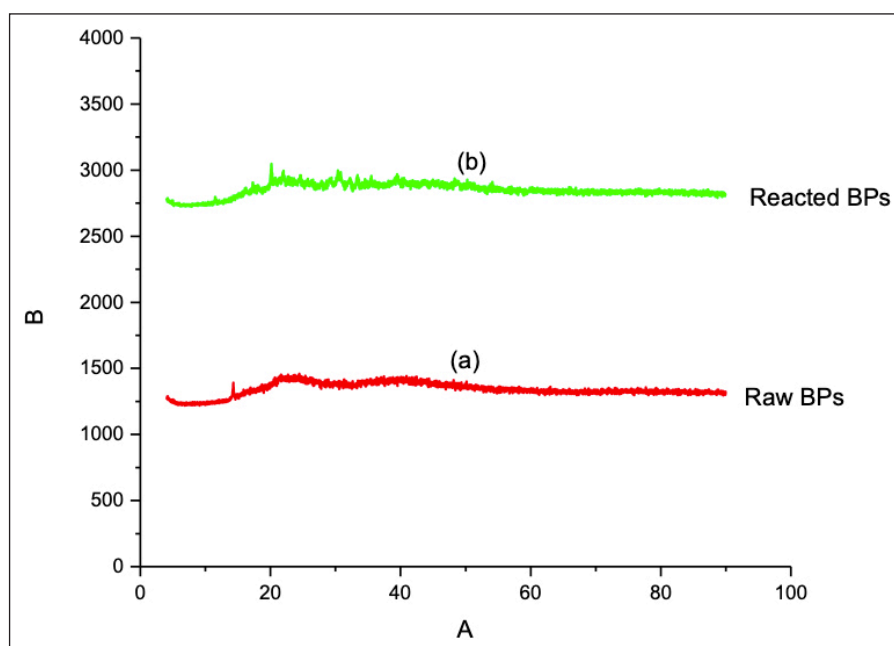


Figure 11. Powder X-ray diffraction results of raw and AMD treated with banana peels.

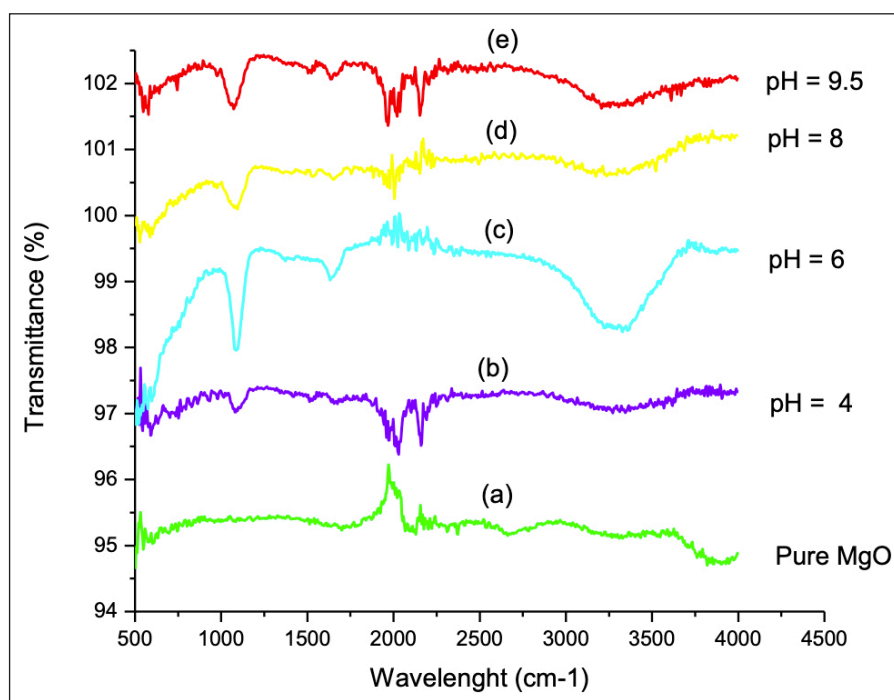


Figure 12. FTIR spectra of pure MgO and sludge materials recovered at different pH gradients.

al group (C=O) stretching vibration as revealed by previous studies [1]. In addition, the sludge recovered at pH 8 and at pH 9.5 interval showed the band at  $600\text{ cm}^{-1}$ , which may correspond to Fe(II) and Fe(III) precipitated during the selective precipitation. The stretching vibration corresponding to band at  $3250\text{ cm}^{-1}$  observed in sludge materials collected at pH 6, pH 8 and pH 9.5 may correspond to Al-OH-Al functional group indicating the presence of aluminum hydroxide  $\text{Al}(\text{OH})_3$  confirming that Al could potentially be recovered from sludge materials collected at those pH gradients, which agree with SEM-EDS results. The peak

at  $1650\text{ cm}^{-1}$  in sludge materials recovered at pH 9.5 may indicate the stretching vibration of Mn-OH-Mn functional group thereby confirming the presence of  $\text{Mn}(\text{OH})_2$ . The findings corroborated with the results obtained in previous studies [1, 43], thereby confirming that many functional groups are formed during selective precipitation of metals in AMD water.

#### FTIR Spectra of BPs Bio-sorbent

The product water collected at pH 9.5 was further polished by means of bio-sorption technique using BPs. Raw and

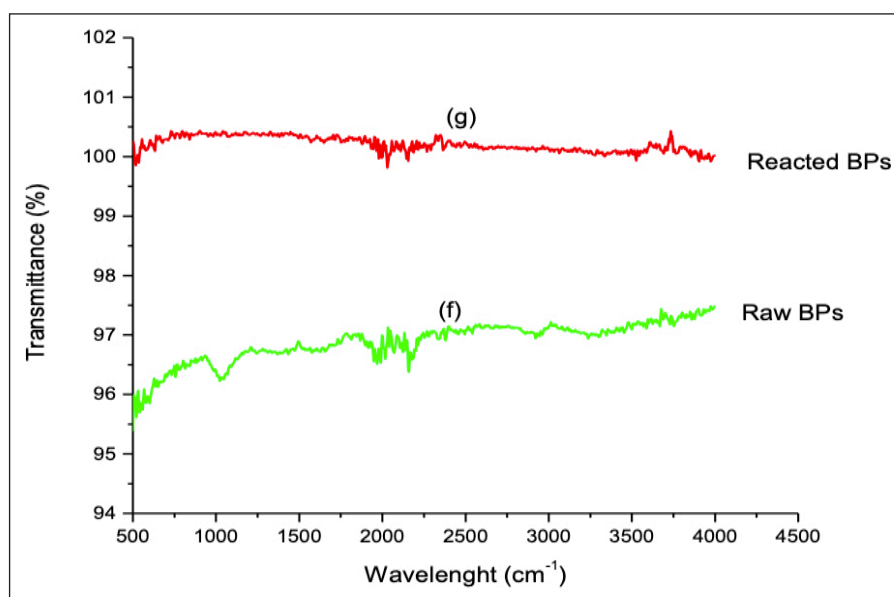


**Figure 13.** FTIR spectra of pure MgO and sludge materials recovered at different pH gradients.

AMD-treated with BPs were analyzed for functional group and the spectra as shown in Figure 13f, g.

The FTIR spectra revealed that BPs contain various functional groups that include hydroxyl, carboxyl and amine groups in its biomass, which facilitate the binding of metal ions from aqueous solution [35, 46]. Both spectra displayed several peaks, which may be attributed to the complex nature of BPs and its tendency to act as bio-sorbent. Bands appearing at  $3750\text{ cm}^{-1}$  for both spectra are indicative of hydroxyl group of polymeric compound, while bands with stretching vibration at  $2000\text{ cm}^{-1}$  may be attributed to carbonyl group (C=O) and carboxyl group (-COOH) thereby confirming the findings reported by Arifiyana and Devianti. [92]. The spectrum of raw BPs (Fig. 13f) displayed a peak at  $1000\text{ cm}^{-1}$  and  $3000\text{ cm}^{-1}$  indicating the presence of hydroxyl and carboxyl groups, respectively. Contrary to the spectrum of raw BPs, the spectrum of AMD treated with BPs (Fig. 13b) revealed significant reduction of intensity, which led to the complete disappearance of peaks at  $1000\text{ cm}^{-1}$  and  $3000\text{ cm}^{-1}$ . The complete disappearance of these peaks in AMD treated with BPs may be attributed to the effective adsorption of pollutants onto the bio-sorbent surface. This finding corroborated with the results obtained by Rao et al. [93] and by Badessa et al. [94] when the used BPs based bio-sorbent for the removal of heavy metals from synthetic solutions and BPs powder for effective removal of chromium from wastewater, respectively.

#### Thermogravimetric Analysis Results

The thermal decomposition of BPs was studied using TGA analysis and the results revealed that raw and treated with BPs displayed the same patterns with two mass loss but at different temperature as shown in Figure 14a, b.

From Figure 14, it follows that the first mass loss happened between 3 and 14 and between 3 and 22 °C for raw and AMD treated with BPs, respectively. This may

correspond to the loss of biomass as a result of moisture removal and some low molecular volatile compounds from the BPs biomass [95, 96]. The mild change in % of weight between raw and treated with BPs may be attributed to the presence of pollutants (chemical species) in AMD treated with BPs. In fact, following the contact of BPs with AMD water for an optimum contact time of 300 min, chemical species are adsorbed, and their degradation require high temperature, and this may explain the mild change in % between the raw and AMD treated with BPs. In the second mass loss (14 and 60 °C) for raw BPs (Fig. 14a) and between 23 and 85 °C for AMD treated with BPs (Fig. 14b), the 2 curves remain similar in nature but the slope of curve of raw BPs is steeper and this may indicate a faster conversion and mass loss with increasing temperature [96, 97]. The second mass loss in raw BPs may be attributed to the thermal degradation of cellulose, lignin and hemicellulose thereby confirming the finding reported by Kabenge et al. [98], when they studied the TGA analysis of pure BPs. The finding also revealed the continuous mass loss in AMD treated with BPs. Given that pollutants and specifically metals are difficult to decay, this may be indicating the presence of metals in AMD treated with BPs [95, 96]. Metals doping or impurities in the pre-treated AMD water were adsorbed by BPs and as result, require high temperature for their degradation.

#### Zeta Potential of Bio-sorbent (BPs)

The zeta potential measurements allow to determine the charge of adsorbent at a particular pH level and the point of zero charge (PZC), the point where the adsorbent has a zero charge [61]. In this study, the zeta potential of raw banana peels (BPs) and AMD treated with RBPs was evaluated in the pH range of 1 to 13 as illustrated in Figure 15.

Figure 15 depicted that the PZC were 2.6 and 2.9 for BPs and RBPs, respectively. It follows that both BPs and RBPs

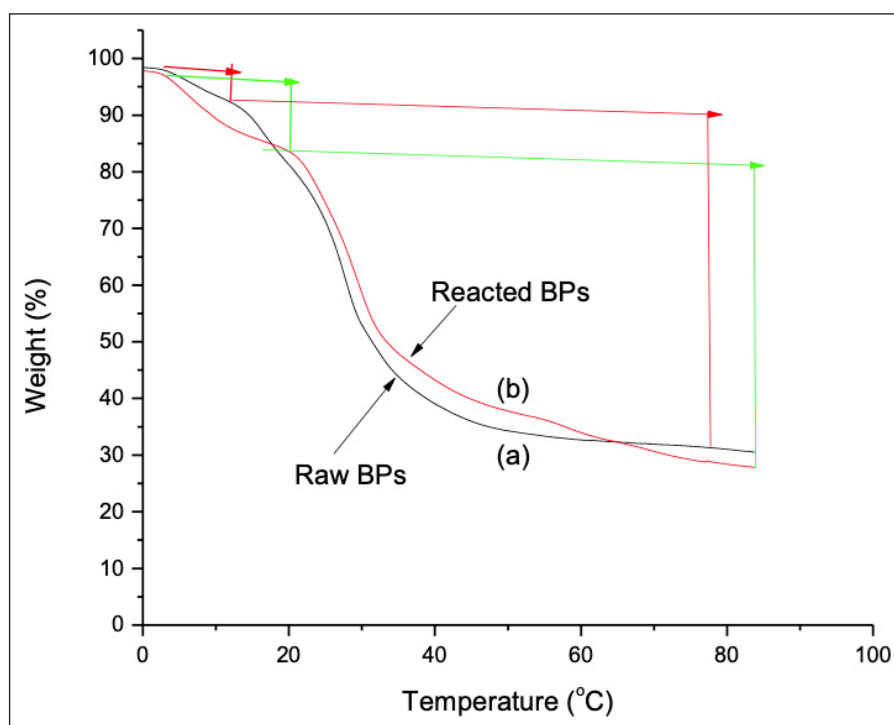


Figure 14. Thermogravimetric results of raw and AMD treated with banana peels.

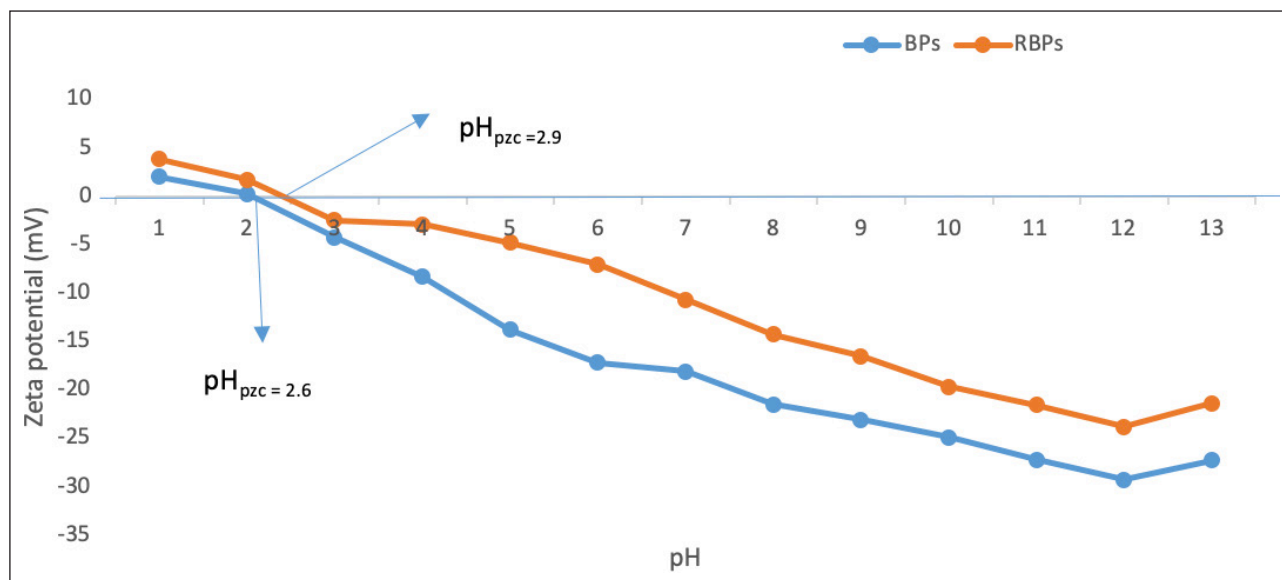


Figure 15. Zeta potentials of raw and AMD treated with banana peels.

assumed negative charge above the PZC. At pH below the PZC, the charge of the solid surface of bio-sorbent is positive and therefore accept protons since the basic group has the possibility to share electrons [99]. However, at pH above the PZC, the surface of the bio-sorbent (BPs) is negatively charged due to the deprotonation of acid groups leading to the interaction with cationic species. The zeta potential has a huge influence on the sorption of chemicals species since those with positive charges will be attracted by the sorbent materials bearing a negative charge while those with negative charges will be attracted by the sorbent materials bearing a positive charge [61, 100, 101]. The narrow differ-

ence between the PZC of BPs and RBPs suggest that after contact of BPs with AMD, the buffering capacity of the BPs increased as reported by previous studies [61].

#### Limit of Detection and Limit of Quantification Results

The LOD or minimum detectable concentration of analyte is the lower amount that can be detected using an analytical standard method while the LOQ is the concentration that can be determined in sample matrix precisely and accurately. The LOD and LOQ of metals (Al, Cu, Fe, Mn, Ni, Zn) and  $\text{SO}_4^{2-}$  were obtained using ICP-OES and IC, respectively and the results are presented in Table 4.



**Table 4.** Limit of detection and limit of quantification of metals and sulphate ions

Chemical species	Coefficient of determination (R <sup>2</sup> )	LOD (mg/L)	LOQ (mg/L)
Al	0.9993	0.001	0.003
Cu	0.9987	0.002	0.006
Fe	0.9997	0.03	0.099
Mn	0.9999	0.01	0.033
Ni	0.9989	0.05	0.166
Zn	0.9992	0.003	0.009
SO <sub>4</sub> <sup>2-</sup>	0.9995	0.116	0.386

LOD: Limit of detection; LOQ: Limit of quantification.

The calibration curve was used to determine the linearity. The coefficient of determination (R<sup>2</sup>) allowed to extrapolate and estimate statistical analysis of unknown concentration of chemicals species where data were considered accurate when R<sup>2</sup> was equal to or close to 1. Linear concentration ranged from 0.1 to 3.5 mg/L was used to test the linearity of calibration curves while the linearity of SO<sub>4</sub><sup>2-</sup> was tested in linear concentration ranged from 10 to 50 mg/L. The R<sup>2</sup> of all determined chemical species are 0.9993, 0.9987, 0.9997, 0.9999, 0.9989, 0.9992, 0.9995 and 1.0000 for Al, Cu, Fe, Mn, Ni, Zn and SO<sub>4</sub><sup>2-</sup>, respectively. This merely means that unknown concentration of each chemical species of concern was extrapolated on the calibration curve with a prediction between 99.23 and 100% for Al, 99.77 and 100% for Cu, 99.97 for Fe, 99.99 for Mn, 99.89 for Ni, 99.82 for Zn and 99.95 for SO<sub>4</sub><sup>2-</sup>.

**Regeneration of BPs Results**

In order to further ensuring environmental pollution control, a regeneration study was conducted since regeneration reduce the need of new adsorbent as well as the disposal of used adsorbent, thereby playing a vital role in environmental pollution control [102]. The reusability of BPs for the polishing of pre-treated AMD water was performed by investigating various adsorption-desorption cycles to assess the RE of bio-sorbent (BPs) in term of number of cycles

that can be conducted to ensure complete regeneration and the results are shown in Figure 16.

Figure 16 depicted that the bio-sorbent RE decrease as well as the number of regeneration cycles increase, and this may be credited to the loss of bio-sorbent mass during filtration. Furthermore, the RE differs from one chemical species to another and this can be attributed to biochemical factors including sizes of chemical species, binding value constant with the BPs, extent of hydration and their tendency to attract electrons as revealed by previous studies [103, 104]. The results corroborated with previous findings proving that BPs can be an efficient bio-sorbent to be used in bio-sorption techniques for water treatment due to the possibility of regeneration of it without high impact on it bio-sorption capacity.

**CONCLUSION**

The feasibility of selective precipitation of chemical species from AMD using MgO and the polishing of product water using BPs was evaluated. The pH of AMD water was gradually increased and metals were selectively precipitated and optimum condition of 2.3 g:2000 mL (w/v or 2.3:2000 ratio), was applied to reach the maximum pH of 9.5 achievable using MgO while the optimum condition for bio-sorption step was 1:500 mL or 1:500 ratio for a 300 min of equilibration as reported by Mahlangu et al. [47] were applied in this study. The chemical treatment using selective precipitation led to an increase of pH from 1.7 to 9.5, significant reduction of EC, TDS, SO<sub>4</sub><sup>2-</sup> and metals (Al, Cu, Fe, Mn, Ni and Zn). The analysis of sludge materials recovered at different pH gradients revealed that chemical species were selectively precipitated, thereby confirming that valuable chemical species including Al, Cu, Fe, Mn, Ni, Zn and CaSO<sub>4</sub>.2H<sub>2</sub>O can be recovered using selective precipitation with Fe and CaSO<sub>4</sub>.2H<sub>2</sub>O being the major chemical species as confirmed by their high percentage in EDS results. The polishing of product water using BPs further increased the pH from 9.5 to 10 leading to more removal of pollutants with an overall RE as follows: Al (100%), Cu (100%), Zn (100%) > Fe (99.99%), Mn (99.99%) > Ni (99.93%) > EC (95%) > SO<sub>4</sub><sup>2-</sup> (90%) > TDS (86%). The selective precipitation using MgO allowed to recover sludge

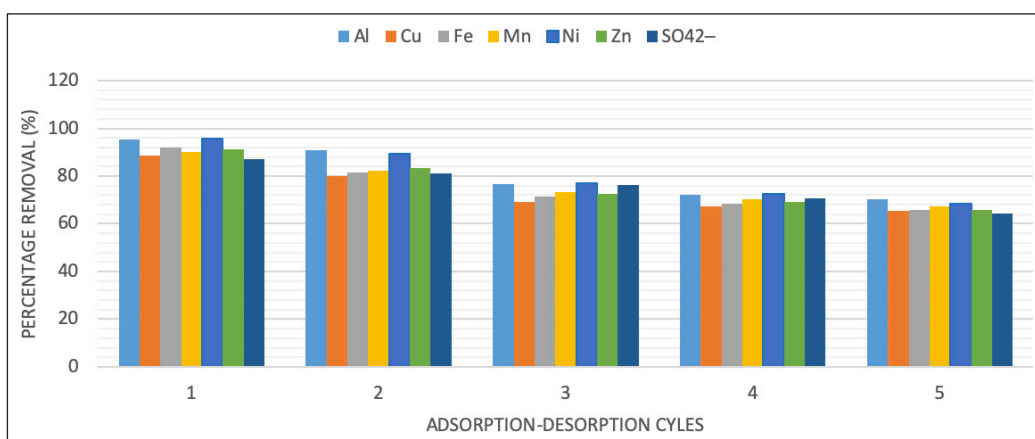


**Figure 16.** Adsorption-desorption cycles of chemicals species of concern.

rich in metals at different pH gradient and substantially contributed to overall removal of chemical species with RE in the following order: Fe (99.96%) > Cu (99.7%) > Al (99.36%) > Ni (99.34%) > Zn (99%) > Mn (97.47%) > EC (90%) > TDS (78%) >  $\text{SO}_4^{2-}$  (75%), while the bio-sorption using BPs for 300 min accounted for a minor fraction of overall chemical species removal with RE as follows:  $\text{SO}_4^{2-}$  (15%) > TDS (8%) > EC (5%) > Mn (2.53%) > Zn (1%) > Ni (0.66%) > Al (0.64%) > Cu (0.4%) > Fe (0.03%). This study revealed the efficiency of MgO in selective precipitation of metals from AMD; thereby, reducing pollutants concentration and the polishing potential of BPs. Overall, this study proved that AMD can be valorized through selective precipitation and recovery of metals using MgO and polish the product water using BPs to reclaim drinking water standards. This will go a long way to implement CEA in both mining and agricultural industries thereby controlling environmental pollution associated with the above mentioned industries. However, the technology presents some disadvantage such as the coloration of product water after polishing using BPs but calcinated BPs can be used to polish the pre-treated AMD water in order to avoid coloration of product water.

## ACKNOWLEDGEMENTS

The authors would like to acknowledge the Faculty of Science, University of Johannesburg for postdoctoral scholarship for NB. The project is supported by the Water Research Commission (WRC) of South Africa, Project Number C2022/2023-00933. We acknowledge the University of Johannesburg Research Centre for Synthesis and Catalysis and Spectrum for the facility.

## DATA AVAILABILITY STATEMENT

The author confirm that the data that supports the findings of this study are available within the article. Raw data that support the finding of this study are available from the corresponding author, upon reasonable request.

## CONFLICT OF INTEREST

The author declared no potential conflicts of interest with respect to the research, authorship, and/or publication of this article.

## USE OF AI FOR WRITING ASSISTANCE

Not declared.

## ETHICS

There are no ethical issues with the publication of this manuscript.

## REFERENCES

- [1] V. Masindi, J. G. Ndiritu, and J. P. Maree, "Fractional and step-wise recovery of chemical species from acid mine drainage using calcined cryptocrystalline magnesite nano-sheets: An experimental and geochemical modelling approach," *Journal of Environmental Chemical Engineering*, Vol. 6(2), pp.1634–1650, 2018. [\[CrossRef\]](#)
- [2] N. Beauclair, V. Masindi, T. A. M. Makudali, M. Tekere, and I. M. Ndoh, "Assessing the performance of horizontally flowing subsurface wetland equipped with *Vetiveria zizanioides* for the treatment of acid mine drainage," *Advances in Environmental Technology*, Vol. 8(2), pp. 103–127, 2022.
- [3] V. Masindi, M. S. Osman, and R. "Shingwenyana, valorization of acid mine drainage (AMD): A simplified approach to reclaim drinking water and synthesize valuable minerals-Pilot study," *Journal of Environmental Chemical Engineering*, Vol. 7(3), Article 103082, 2019. [\[CrossRef\]](#)
- [4] J. G. Skousen, P. F. Ziemkiewicz, and L. M. McDonald, "Acid mine drainage formation, control and treatment: Approaches and strategies," *Extractive Industries and Society*, Vol. 6(2), pp. 241–249, 2019. [\[CrossRef\]](#)
- [5] K. Moeng, "Community perceptions on the health risks of acid mine drainage: the environmental justice struggles of communities near mining fields," *Environmental Development Sustainable*, Vol. 21, pp. 2619–2640, 2019. [\[CrossRef\]](#)
- [6] V. Akinwekomi, J. P. Maree, C. Zvinowanda, and V. Masindi, "Synthesis of magnetite from iron-rich mine water using sodium carbonate," *Journal of Environmental Chemical Engineering*, Vol. 5(3), pp. 2699–2707, 2017. [\[CrossRef\]](#)
- [7] D. K. Nordstrom, D. W. Blowes, and C. J. Ptacek, "Hydrogeochemistry and microbiology of mine drainage: An update," *Applied Geochemistry*, Vol. 57, pp. 3–16, 2015. [\[CrossRef\]](#)
- [8] A. Teresa, C. Francisco, A. Catarina, R. Loayza-Muro, S. Bruna, J. Diaz-Curiel..., and J.A. Grande, "Extremely acidic eukaryotic (Micro) organisms: Life in acid mine drainage polluted environments — mini-review," *International Journal of Environmental Research and Public Health*, Vol. 19(1), pp. 1–13, 2022. [\[CrossRef\]](#)
- [9] M. A. Caraballo, T. S. Rötting, F. Macías, J. M. Nieto, and C. Ayora, "Field multi-step limestone and MgO passive system to treat acid mine drainage with high metal concentrations," *Applied Geochemistry*, Vol. 24(12), pp. 2301–11, 2009. [\[CrossRef\]](#)
- [10] T. S. Rötting, M. A. Caraballo, J. A. Serrano, C. Ayora, and J. Carrera, "Field application of calcite Dispersed Alkaline Substrate (calcite-DAS) for passive treatment of acid mine drainage with high Al and metal concentrations," *Applied Geochemistry*, Vol. 23(6), pp. 1660–1674, 2008. [\[CrossRef\]](#)
- [11] O. Y. Toraman and M. S. Delibalta, "Ultrasonic desulfurization of low rank Turkish coal using various chemical reagents," *Journal of Multidisciplinary Engineering Sciences and Technology*, Vol. 3(4), pp. 4621–4623, 2016.
- [12] V. Masindi, M. W. Gitari, H. Tutu, and M. Debeer, "Efficiency of ball milled South African bentonite clay for remediation of acid mine drainage," *Journal of Water Process Engineering*, Vol. 8, pp. 227–240, 2015. [\[CrossRef\]](#)

- [13] C. O. A. Turingan, K. S. Cordero, A. L. Santos, G. S. L. Tan, R. D. Alorro, and A. H. Orbecido. "Acid mine drainage treatment using a process train with laterite mine waste, concrete waste, and limestone as treatment media, *Water*, Vol. 14(7), pp. 1–21, 2022. [\[CrossRef\]](#)
- [14] B. Nguegang, V. Masindi, T. A. M. Msagati, and M. Tekere. "The treatment of acid mine drainage using vertically flowing wetland: Insights into the fate of chemical species," *Minerals*, Vol. 11(5), pp. 1–24, 2021. [\[CrossRef\]](#)
- [15] B. Nguegang, V. Masindi, T. A. M. Msagati, and T. Memory, "Passive remediation of acid mine drainage using phytoremediation: Role of substrate, plants, and external factors in inorganic contaminants removal," Wiley, 2023.
- [16] L. Marchand, M. Mench, D. L. Jacob, and M. L. Otte, "Metal and metalloid removal in constructed wetlands, with emphasis on the importance of plants and standardized measurements: A review," *Environmental Pollution*, Vol. 158(12), pp. 3447–3461, 2010. [\[CrossRef\]](#)
- [17] S. Alemdag, E. Akaryali, and M. A. Gücer, "Prediction of mine drainage generation potential and the prevention method of the groundwater pollution in the Gümüşköy (Kütahya) mineralization area, NW Turkey," *Journal of Mountain Sciences*, Vol. 17, pp. 2387–2404, 2020. [\[CrossRef\]](#)
- [18] E. Akaryalı, M. A. Gücer, and S. Alemdağ, "Atık barajı rezervuarı ve cevher stok alanlarında asit maden drenajı (AMD) oluşumunun değerlendirilmesi: Gümüşhane örneği atık barajı rezervuarı ve cevher stok alanlarında asit maden drenajı (amd) oluşumunun değerlendirilmesi: Gümüşhane örneği," *Journal of Natural Hazard and Environmentno*, Vol. 4(2), pp. 192–209, 2018. [\[CrossRef\]](#)
- [19] M. A. Gücer, S. Alemdağ, and E. Akaryali, "Assessment of acid mine drainage formation using geochemical and static tests in Mutki (Bitlis, SE Turkey) mineralization area," *Turkish Journal of Earth Sciences* Vol. 29, pp. 1189–1210, 2020. [\[CrossRef\]](#)
- [20] G. H. Berghorn and G. R. Hunzeker, "Passive treatment alternatives for remediating abandoned- mine drainage," *Remediation*, Vol. 11(3), pp. 111–127, 2001. [\[CrossRef\]](#)
- [21] J. D. Kiiskila, D. Sarkar, K. A. Feuerstein, and R. Datta, "A preliminary study to design a floating treatment wetland for remediating acid mine drainage-impacted water using vetiver grass (*Chrysopogon zizanioides*)," *Environmental Sciences and Pollution Research*, Vol. 24, pp. 27985–27993, 2017. [\[CrossRef\]](#)
- [22] D. Kiiskila, D. Sarkar, S. Panja, S. V. Sahi, and R. Datta, "Remediation of acid mine drainage-impacted water by vetiver grass (*Chrysopogon zizanioides*): A multi-scale long-term study," *Ecological Engineering*, Vol. 129, pp. 97–108, 2019. [\[CrossRef\]](#)
- [23] B. G. Lottermoser and P. M. Ashley, "Trace element uptake by *Eleocharis equisetina* (spike rush) in an abandoned acid mine tailings pond, northeastern Australia: Implications for land and water reclamation in tropical regions," *Environmental Pollution*, Vol. 159(10), pp. 3028–3035, 2011. [\[CrossRef\]](#)
- [24] B. Nguegang, V. Masindi, T. A. M. Msagati, and M. Tekere, "Effective treatment of acid mine drainage using a combination of MgO-nanoparticles and a series of constructed wetlands planted with *Vetiveria zizanioides*: A hybrid and stepwise approach," *Journal of Environmental Management*, Vol. 310, Article 114751, 2022. [\[CrossRef\]](#)
- [25] B. Nguegang, V. Masindi, T. T.A.M. Msagati, M. Tekere, and A.A Ambushe, "Hybrid treatment of acid mine drainage using a combination of mgo-nps and a series of constructed wetland planted with *vetiveria zizanioides*," 35<sup>th</sup> International Conference on Chemical, Biological and Environmental Engineering (ICCBEE-22) Nov. 28–29, 2022 Johannesburg (South Africa), 2022.
- [26] V. Masindi, M. S. Osman, and A. M. Abu-Mahfouz, "Integrated treatment of acid mine drainage using BOF slag, lime/soda ash and reverse osmosis (RO): Implication for the production of drinking water," *Desalination*, Vol. 424, pp. 45–52, 2017. [\[CrossRef\]](#)
- [27] T. J. Hengen, M. K. Squillace, A. D. O'Sullivan, and J. J. Stone, "Life cycle assessment analysis of active and passive acid mine drainage treatment technologies," *Resources Conservation and Recycling*. Vol. 86, pp. 160–167, 2014. [\[CrossRef\]](#)
- [28] E. MacIngova, and A. Luptakova, "Recovery of metals from acid mine drainage," *Chemical Engineering Transactions*, Vol. 28, pp. 109–114, 2012.
- [29] A. N. Shabalala, S. O. Ekolu, S. Diop, and Solomon, "Pervious concrete reactive barrier for removal of heavy metals from acid mine drainage – Column study" *Journal of Hazardous Materials*, Vol. 323(Pt B), pp. 641–653, 2017. [\[CrossRef\]](#)
- [30] A. Khan, (2014). "Ion exchange- A treatment option for acid mine drainage (Master's thesis)." Available from NTNU Open. 2002.
- [31] O. Agboola, "The role of membrane technology in acid mine water treatment: A review," *Korean Journal of Chemical Engineering*, Vol. 36, pp. 1389–1400, 2019. [\[CrossRef\]](#)
- [32] A. Munyengabe, C. Zvinowanda, J. Ramontja, and J.N. Zvimba, "Effective desalination of acid mine drainage using an advanced oxidation process: Sodium ferrate (VI) salt," *Water (Switzerland)*, Vol. 13(19), Article 2619, 2021. [\[CrossRef\]](#)
- [33] H. J. Choi, "Biosorption of heavy metals from acid mine drainage by modified sericite and microalgae hybrid system," *Water Air Soil Pollution*, Vol. 226(6), Article 185, 2015. [\[CrossRef\]](#)
- [34] E. Y. Seo, Y. W. Cheong, G. J. Yim, K. W. Min, and J. N. Geroni, "Recovery of Fe, Al and Mn in acid coal mine drainage by sequential selective precipitation with control of pH," *Catena*, Vol. 148(Pt 1), pp.11–16, 2017. [\[CrossRef\]](#)
- [35] E. Torres, "Biosorption: A review of the latest advances," *Processes*, Vol. 8(12), Article 1584, 2020. [\[CrossRef\]](#)
- [36] M. Danouche, H. El Arroussi, W. Bahafid, and N. El Ghachtouli, "An overview of the biosorption mech-

- anism for the bioremediation of synthetic dyes using yeast cells,” *Environmental Technology Reviews*, Vol. 10(1), pp. 58–76, 2020. [CrossRef]
- [37] R. J. Nathan, C. E. Martin, D. Barr, R. J. Rosengren, “Simultaneous removal of heavy metals from drinking water by banana, orange and potato peel beads: A study of biosorption kinetics,” *Applied Water and Sciences*, Vol. 11(7), Article 116, 2021. [CrossRef]
- [38] D. Ramutshatsha-Makhwedzha, R. Mbaya, and M. L. Mavhungu, “Application of activated carbon banana peel coated with Al<sub>2</sub>O<sub>3</sub>-Chitosan for the adsorptive removal of lead and cadmium from wastewater,” *Materials*, Vol. 15(3), Article 869, 2022. [CrossRef]
- [39] S. Park, and M. Lee, “Removal of copper and cadmium in acid mine drainage using Ca-alginate beads as biosorbent,” *Geosciences Journal*, Vol. 21, pp. 373–383, 2017. [CrossRef]
- [40] L. F. Leon-Fernandez, H. L. Medina-Díaz, O. G. Pérez, R. Romero, J. Villasenor, and F. J. Fernández-Morales, “Acid mine drainage treatment and sequential metal recovery by means of bioelectrochemical technology,” *Journal of Chemical Technology and Biotechnology*, Vol. 96(6), pp.1543–1552, 2021. [CrossRef]
- [41] T. Chen, B. Yan, C. Lei, and X. Xiao, “Pollution control and metal resource recovery for acid mine drainage,” *Hydrometallurgy*, Vol. 147–148, pp.112–119, 2014. [CrossRef]
- [42] C. Oh, Y. S. Han, J. H. Park, S. Bok, Y. Cheong, G. Yim, and S. Ji, “Field application of selective precipitation for recovering Cu and Zn in drainage discharged from an operating mine,” *Sciences of the Total Environment*, Vol. 557–558, pp. 212–220, 2016. [CrossRef]
- [43] A. Navarro, M. I. Martínez da Matta, “Application of magnesium oxide for metal removal in mine water treatment,” *Sustainability*, Vol. 14(23), Article 15857, 2022. [CrossRef]
- [44] A. Sulaiman, A. Othman, and Ibrahim I, “The use of magnesium oxide in acid mine drainage treatment,” *Materials Today: Proceeding*, Vol. 5(10), pp. 21566–21573, 2018. [CrossRef]
- [45] E. Mamakoa, V. Masindi, H. Neomagus, “Comparison of MgO and MgCO<sub>3</sub> in the treatment of Acid Mine Drainage.” 2020. <http://eares.org/siteadmin/upload/5831EAP1120216.pdf>. data/QCL Accessed on Apr 24, 2023.
- [46] A. Ali, “Removal of Mn(II) from water using chemically modified banana peels as efficient adsorbent,” *Environmental Nanotechnology Monitoring and Management*, Vol. 7, pp. 57–63, 2017. [CrossRef]
- [47] J. M. Mahlangu, G. S. Simate, and M. Beer, “Adsorption of Mn<sup>2+</sup> from the acid mine drainage using banana peel,” *International Journal of Water and Wastewater Treatment*, Vol. 4(1), pp. 1–9, 2018. [CrossRef]
- [48] P. Pourhakkak, A. Taghizadeh, M. Taghizadeh, M. Ghaedi, and S. Haghdoost, “Chapter 1- Fundamentals of Adsorption Technology,” Vol. 33, pp. 1–70, 2021. [CrossRef]
- [49] W. J. Shin, H. S. Shin, J. H. Hwang, and K. S. Lee, “Effects of filter-membrane materials on concentrations of trace elements in acidic solutions,” *Water (Switzerland)*, Vol. 12(12), Article 3497, 2020. [CrossRef]
- [50] American Public Health Association (APHA), “American Water Works Association) Water Environment Federation, Stand. Methods Exam. Water Wastewater,” American Public Health Association, 2002.
- [51] A. B. M. Helal Uddin, R. S. Khalid, M. Alaama, A. M. Abdulkader, A. Kasmuri, S. A. Abbas, “Comparative study of three digestion methods for elemental analysis in traditional medicine products using atomic absorption spectrometry,” *Journal of Analytical Sciences and Technology*, Vol. 1, Article 6, 2020.
- [52] H. Hernández-Mendoza, M. Mejuto, A. I. Cardona, A. García-Álvarez, R. Millán, and A. Yllera, “Optimization and validation of a method for heavy metals quantification in soil samples by inductively coupled plasma sector field mass spectrometry (ICP-SFMS),” *American Journal of Analytical Chemistry*, Vol. 4, Article 10b, 2013. [CrossRef]
- [53] H. B. Vaziri, Y. Shekarian, and M. Rezaee, “Selective precipitation of rare earth and critical elements from acid mine drainage - Part I: Kinetics and thermodynamics of staged precipitation process,” *Resources Conservation and Recycling*, Vol.188, Article 106654, 2023. [CrossRef]
- [54] C. Rodríguez, E. Leiva-Aravena, J. Serrano, and E. Leiva, “Occurrence and removal of copper and aluminum in a stream confluence affected by acid mine drainage,” *Water (Switzerland)*, Vol. 10(4), Article 516, 2018. [CrossRef]
- [55] J. S. España, “Chapter 7- The behavior of iron and aluminum in acid mine drainage. Speciation, mineralogy, and environmental significance,” *Thermodynamics, Solubility and Environment Issues*, pp.137–150, 2007. [CrossRef]
- [56] M. Santander-Muñoz, P. Cardozo-Castillo, and L. Valderrama-Campusano, “Removal of sulfate ions by precipitation and flotation, Engineering Investigation,” *Chemical, Food, and Environmental Engineering*, Vol. 41, Article 3, 2021. [CrossRef]
- [57] A. G. Reiss, G. Ittai, Y. O. Rosenberg, I. J. Reznik, A. Luttge, S. Emmanuel, and J. Ganor, “Gypsum precipitation under saline conditions: Thermodynamics, kinetics, morphology, and size distribution,” *Minerals*. Vol. 11(2), Article 141, 2021. [CrossRef]
- [58] R. M. Freitas, T. A. G. Perilli, and A. C. Q. Ladeira, “Oxidative precipitation of manganese from acid mine drainage by potassium permanganate,” *Journal of Chemistry*, Vol. 2013, Article 287257, 2013. [CrossRef]
- [59] M. Hove, R. P. Van Hille, and A. E. Lewis. “Mechanisms of formation of iron precipitates from ferrous

- solutions at high and low pH,” *Chemical Engineering Sciences*, Vol. 63(6), 1626–1635, 2008. [\[CrossRef\]](#)
- [60] V. Masindi, M. W. Gitari, H. Tutu, M. De Beer, “Passive remediation of acid mine drainage using cryptocrystalline magnesite: A batch experimental and geochemical modelling approach,” *Water SA*, Vol. 41(5), pp. 677–682, 2015. [\[CrossRef\]](#)
- [61] F. O. Afolabi, P. Musonge, and B. F. Bakare, “Adsorption of copper and lead ions in a binary system onto orange peels: Optimization, equilibrium and kinetic study,” *Sustainability*, Vol. 14(17), Article 10860, 2022. [\[CrossRef\]](#)
- [62] H. Mohd, J. Roslan, S. Saallah, E. Munsu, N. Shaera, and W. Pindi, “Banana peels as a bioactive ingredient and its potential application in the food industry,” *Journal of Function Foods*, Vol. 92, Article 105054, 2021. [\[CrossRef\]](#)
- [63] M. M. Miranda, J. M. Bielicki, S. Chun, and C. M. Cheng, “Recovering rare earth elements from coal mine drainage using industrial byproducts: Environmental and economic consequences,” *Environmental Engineering Sciences*, Vol. 39(9), pp. 770–783, 2022. [\[CrossRef\]](#)
- [64] D. F. Parsons, and A. Salis, “The impact of the competitive adsorption of ions at surface sites on surface free energies and surface forces,” *Journal of Chemistry and Physics*, Vol. 142(13), Article 134707, 2015. [\[CrossRef\]](#)
- [65] S. Indah, D. Helard, T. Edwin, and R. Pratiwi, “Utilization of pumice from Sungai Pasak, West Sumatera, Indonesia as low-cost adsorbent in removal of manganese from aqueous solution,” *AIP Conference Proceeding*, Vol. 1823(1), pp.1823–1830, 2017. [\[CrossRef\]](#)
- [66] A. Mohan, “Study of sugarcane bagasse and orange peel as adsorbent for treatment of industrial effluent contaminated with nickel,” *International Resources Journal of Engineering and Technology*, Vol. 6, pp. 4725–4731, 2019.
- [67] M. Negroiu, A. T. Anca, E. Matei, M. Râpă, C. I. Covaliu, A. M. Predescu..., and C. Predescu, “Novel adsorbent based on banana peel waste for removal of heavy metal ions from synthetic solutions,” *Materials*, Vol. 14(14), pp. 3946–3958. [\[CrossRef\]](#)
- [68] M. Abd-Elaziz, M. G. Taha, M. Gahly, and H. T. Hefnawy, “Removal of Fe<sup>3+</sup> and Pb<sup>2+</sup> ions from aqueous solutions by adsorption using banana peels,” *Zagazig Journal of Agricultural Resources*, Vol. 49(4), pp. 853–864, 2022. [\[CrossRef\]](#)
- [69] N. R. Molaudzi, and A. A. Ambushe, “Sugarcane bagasse and orange peels as low-cost biosorbents for the removal of lead ions from contaminated,” *Water*, Vol. 14(21), Article 3395, 2022. [\[CrossRef\]](#)
- [70] G. Teng, X. Yuen, and X. Fen, “Adsorption of pollutants in wastewater via biosorbents, nanoparticles and magnetic biosorbents: A review,” *Environmental Resources*, Vol. 212(Pt B), Article 113248, 2022. [\[CrossRef\]](#)
- [71] M. Bilal, I. Ihsanullah, M. Younas, and M. H. Shah, “Recent advances in applications of low-cost adsorbents for the removal of heavy metals from water: A critical review,” *Separation and Purification Technology*, Vol. 278, Article 119510, 2021. [\[CrossRef\]](#)
- [72] K. Khairiah, E. Frida, K. Sebayang, P. Sinuhaji, and S. Humaidi, “Data on characterization, model and adsorption rate of banana peel activated carbon (*Musa Acuminata*) for adsorbents of various heavy metals (Mn, Pb, Zn, Fe), *Data in Brief*, Vol. 39, Article 107611, 2021. [\[CrossRef\]](#)
- [73] R. M. Mohamed, N. Hashim, A. Suhaila, N. Abdullah, A. Mohamed, M. A. A. Daud..., and S. Abdullah, “Adsorption of heavy metals on banana peel bioadsorbent,” *Journal of Physics*, Vol. 1521, Article 012014, 2020. [\[CrossRef\]](#)
- [74] Y. Zheng, X. Zhang, Z. Bai, and Z. Zhang, “Characterization of the surface properties of MgO using paper spray mass spectrometry,” *Rapid Commun Mass Spectrum*, Vol. 30(S1), pp. 217–225, 2016. [\[CrossRef\]](#)
- [75] X. Wei, R. C. Viadero, and K. M. Buzby, “Recovery of iron and aluminum from acid mine drainage by selective precipitation,” *Environmental Engineering Sciences*, Vol. 22(6), 745–755, 2005. [\[CrossRef\]](#)
- [76] Y. Li, Z. Xu, H. Ma, and A. S. Hursthouse, “Removal of manganese(II) from acid mine wastewater: A review of the challenges and opportunities with special emphasis on mn-oxidizing bacteria and microalgae,” *Water (Switzerland)*, Vol. 11(12), Article 2493. [\[CrossRef\]](#)
- [77] R. M. Salim, A. Jalal, K. Chowdhury, and R. Rayathulhan, “Biosorption of Pb(II) and Cu(II) from aqueous solution using banana peel powder Biosorption of Pb and Cu from aqueous solution using banana peel powder,” *Desalination and Water Treatment*, Vol. 57(1), pp. 303–314, 2016. [\[CrossRef\]](#)
- [78] Y. Zhang, S. Liao, Y. Fan, J. Xu, and F. Wang, “Chemical reactivities of magnesium nanopowders,” *Journal of Nanoparticle Research*, Vol. 3(1), pp. 23–26, 2001. [\[CrossRef\]](#)
- [79] I. Shancita, N. G. Vaz, G. D. Fernandes, A. J. A. Aquino, D. Tunega, and M. L. Pantoya, “Regulating magnesium combustion using surface chemistry and heating rate,” *Combustion and Flame*, Vol. 226, pp. 419–429, 2021. [\[CrossRef\]](#)
- [80] R. Coetzee, C. Dorfling, and S. M. Bradshaw, “Characterization of precipitate formed during the removal of iron and precious metals from sulphate leach solutions,” *Journal of Southern African Institute of Minerals and Metallurgic*, Vol. 117, pp. 771–778, 2017. [\[CrossRef\]](#)
- [81] W. M. Gitari, L. F. Petrik, O. Etchebers, D. L. Key, E. Iwuoha, and C. Okujeni, “Passive neutralisation of acid mine drainage by fly ash and its derivatives: A column leaching study,” *Fuel*, Vol. 87(8–9), pp. 1637–1650, 2008. [\[CrossRef\]](#)
- [82] V. Masindi, 1A novel technology for neutralizing acidity and attenuating toxic chemical species from

- acid mine drainage using cryptocrystalline magnetite tailings,” *Journal of Water Process Engineering*, Vol. 10, pp. 67–77, 2016. [\[CrossRef\]](#)
- [83] R. Khosravi, R. Fatahi, H. Siavoshi, and F. Molaei, “Recovery of manganese from zinc smelter slag,” *American Journal of Engineering Applied Sciences*, Vol. 13(4), pp. 748–758, 2020. [\[CrossRef\]](#)
- [84] D. Gopi, K. Kanimozhi, N. Bhuvaneshwari, J. Indira, and L. Kavitha, “Novel banana peel pectin mediated green route for the synthesis of hydroxyapatite nanoparticles and their spectral characterization,” *Spectrochimica Acta Part A Molecular and Biomolecular Spectroscopy*, Vol. 118, pp. 589–597, 2014. [\[CrossRef\]](#)
- [85] J. R. Memon, S. Q. Memon, M. I. Bhangar, G. Z. Memon, A. El-Turki, and G. C. Allen, “Characterization of banana peel by scanning electron microscopy and FT-IR spectroscopy and its use for cadmium removal. *Colloids Surfaces B Biointerfaces*,” Vol. 66, pp. 260–265, 2008. [\[CrossRef\]](#)
- [86] G. Balakrishnan, R. Velavan, B. K. Mujasam, and E.H. Raslan, “Microstructure, optical and photocatalytic properties of MgO nanoparticles,” *Results in Physics*, Vol. 16, Article 103013, 2020. [\[CrossRef\]](#)
- [87] J. T. Richardson, R. Scates, and M. V. Twigg, “X-ray diffraction study of nickel oxide reduction by hydrogen,” *Applied Catalyst A General*, Vol. 246, pp. 137–150, 2003. [\[CrossRef\]](#)
- [88] H. Tibolla, F. M. Pelissari, J. T. Martins, A. A. Vicente, and F.C. Menegalli, “Cellulose nanofibers produced from banana peel by chemical and mechanical treatments: Characterization and cytotoxicity assessment,” *Food Hydrocoll*, Vol. 75, pp.192–201, 2018. [\[CrossRef\]](#)
- [89] S. Mishra, B. Prabhakar, P. S. Kharkar, and A. M. Pethe, “Banana peel waste: An emerging cellulosic material to extract nanocrystalline cellulose,” *ACS Omega*, Vol. 8(1), pp.1140–1145, 2023. [\[CrossRef\]](#)
- [90] N. K. Nga, N. T. Thuy Chau, and P. H. Viet, “Preparation and characterization of a chitosan/MgO composite for the effective removal of reactive blue 19 dye from aqueous solution,” *Journal of Sciences and Advances Materials Devices*, Vol. 5(1), pp. 65–72, 2020. [\[CrossRef\]](#)
- [91] N. Sutradhar, S. Apurba, S. K. Pahari, P. Pal, C.H. Bajaj, I. Mukhopadhyay, and A. B. Panda, “Controlled synthesis of different morphologies of MgO and their use as solid base catalysts,” *Journal of Physics and Chemistry*, Vol. 115(25), pp.12308–12316, 2011. [\[CrossRef\]](#)
- [92] D. Arifiyana, and V. A. Devianti, “Biosorption of Fe(II) ions from aqueous solution using banana peels (*Musa a cuminata*)” *Jurnal Kimia Dan Pendidikan Kimia*, Vol. 6(2), pp. 206–215, 2021. [\[CrossRef\]](#)
- [93] H. J. Rao, “Characterization studies on adsorption of lead and cadmium using activated carbon prepared from waste tyres,” *Natural Environmental Pollution Technology*, Vol. 20, pp. 561–568, 2021. [\[CrossRef\]](#)
- [94] T. S. Badessa, E. Wakuma, and A. M. Yimer, “Bio-sorption for effective removal of chromium(VI) from wastewater using *Moringa stenopetala* seed powder (MSSP) and banana peel powder (BPP),” *BMC Chemistry*, Vol. 14, Article 71, 2020. [\[CrossRef\]](#)
- [95] R. C. Rivas-Cantu, K. D. Jones, and P. L. Mills, “A citrus waste-based biorefinery as a source of renewable energy: Technical advances and analysis of engineering challenges,” *Waste Management and Resources*, Vol. 31(4), pp. 413–420, 2013. [\[CrossRef\]](#)
- [96] J. R. Ayala, G. Montero, M. A. Coronado, C. Garcia, M. A. Curiel-Alvarez, J. A. Leon..., and D. G. Montes, “Characterization of orange peel waste and valorization to obtain reducing sugars,” *Molecules*, Vol. 26(5), Article 1348, 2021. [\[CrossRef\]](#)
- [97] J. I. Z. Montero, A. S. C. Monteiro, E. S. J. Gontijo, C. C. Bueno, M. A. De Moraes, and A. H. Rosa, “High efficiency removal of As(III) from waters using a new and friendly adsorbent based on sugarcane bagasse and corncob husk Fe-coated biochars,” *Ecotoxicology and Environmental Safety*, Vol. 162, pp. 616–624, 2018. [\[CrossRef\]](#)
- [98] I. Kabenge, G. Omulo, N. Banadda, J. Seay, A. Zziwa, and N. Kiggundu, “Characterization of banana peels wastes as potential slow pyrolysis feedstock,” *Journal of Sustainable Development*, Vol. 11(2), pp.14–24, 2018. [\[CrossRef\]](#)
- [99] F. O. Afolabi, P. Musonge, and B. F. Bakare, “Bio-sorption of a bi-solute system of copper and lead ions onto banana peels: characterization and optimization,” *Journal of Environmental Health Sciences and Engineering*, Vol. 19, pp. 613–624, 2021. [\[CrossRef\]](#)
- [100] F. O. Afolabi, P. Musonge, and B. F. Bakare, “Bio-sorption of copper and lead ions in single and binary systems onto banana peels,” *Cogent Engineering*, Vol. 8(1), Article 1886730, 2021. [\[CrossRef\]](#)
- [101] A. Moubarik, and N. Grimi, “Valorization of olive stone and sugar cane bagasse by-products as biosorbents for the removal of cadmium from aqueous solution,” *Food Research International*, Vol. 73, pp. 169–175, 2015. [\[CrossRef\]](#)
- [102] M. A. Hossain, H. H. Ngo, W. S. Guo, and T. V. Nguyen, “Removal of copper from water by adsorption onto banana peel as bioadsorbent,” *International Journal of Geomate*, Vol. 2, pp. 227–234, 2012. [\[CrossRef\]](#)
- [103] G. Alaa El-Din, A. A. Amer, G. Malsh, and M. Hussein, “Study on the use of banana peels for oil spill removal,” *Alexandria Engineering Journal*, Vol. 57(3), pp. 2061–2068, 2018. [\[CrossRef\]](#)
- [104] R. M. Alghanmi, “ICP-OES determination of trace metal ions after preconcentration using silica gel modified with 1,2-dihydroxyanthraquinone,” *Journal of Chemistry*, Vol. 9, Article 279628, 2012. [\[CrossRef\]](#)